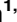



RESEARCH ARTICLE

Atlas of tissue- and developmental stage specific gene expression for the bovine insulin-like growth factor (IGF) system

Mani Ghanipoor-Samami^{1,2}, Ali Javadmanesh^{1,2}[✉], Brian M. Burns³, Dana A. Thomsen^{1,2}, Greg S. Natrass⁴, Consuelo Amor S. Estrella^{1,2}[✉]^{ab}, Karen L. Kind², Stefan Hiendleder^{1,2}^{*}

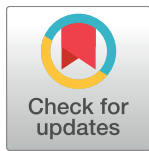
1 Robinson Research Institute, The University of Adelaide, Adelaide, South Australia, Australia, **2** JS Davies Epigenetics and Genetics Group, Davies Research Centre, School of Animal and Veterinary Sciences, Roseworthy Campus, The University of Adelaide, Roseworthy, South Australia, Australia, **3** Centre for Animal Science, Queensland Alliance for Agriculture and Food Innovation, The University of Queensland, Rockhampton, Queensland, Australia, **4** Livestock Systems, South Australian Research and Development Institute (SARDI), Roseworthy, South Australia, Australia

 These authors contributed equally to this work.

[✉] Current address: Department of Animal Science, Faculty of Agriculture, Ferdowsi University of Mashhad, Mashhad, Iran

^{ab} Current address: University of the Philippines, Laguna, Philippines

^{*} stefan.hiendleder@adelaide.edu.au



 OPEN ACCESS

Citation: Ghanipoor-Samami M, Javadmanesh A, Burns BM, Thomsen DA, Natrass GS, Estrella CAS, et al. (2018) Atlas of tissue- and developmental stage specific gene expression for the bovine insulin-like growth factor (IGF) system. *PLoS ONE* 13(7): e0200466. <https://doi.org/10.1371/journal.pone.0200466>

Editor: Thierry Forné, Institute of Molecular Genetics of Montpellier, FRANCE

Received: February 27, 2018

Accepted: June 27, 2018

Published: July 12, 2018

Copyright: © 2018 Ghanipoor-Samami et al. This is an open access article distributed under the terms of the [Creative Commons Attribution License](https://creativecommons.org/licenses/by/4.0/), which permits unrestricted use, distribution, and reproduction in any medium, provided the original author and source are credited.

Data Availability Statement: All relevant data are available from figshare, DOI: [10.4225/55/5b3ae3f80fa4a](https://doi.org/10.4225/55/5b3ae3f80fa4a).

Funding: This work was funded by the JS Davies Bequest with support from the Queensland Government through the Department of Agriculture, Fisheries and Forestry's Reinvestment Fund. AJ and MGS received PhD Scholarships from the Iranian Ministry of Science, Research & Technology and CASE received an Australia

Abstract

The insulin-like growth factor (IGF) axis is fundamental for mammalian growth and development. However, no comprehensive reference data on gene expression across tissues and pre- and postnatal developmental stages are available for any given species. Here we provide systematic promoter- and splice variant specific information on expression of IGF system components in embryonic (Day 48), fetal (Day 153), term (Day 277, placenta) and juvenile (Day 365–396) tissues of domestic cow, a major agricultural species and biomedical model. Analysis of spatiotemporal changes in expression of IGF1, IGF2, IGF1R, IGF2R, IGFBP1-8 and IR genes, as well as lncRNAs H19 and AIRN, by qPCR, indicated an overall increase in expression from embryo to fetal stage, and decrease in expression from fetal to juvenile stage. The stronger decrease in expression of lncRNAs (average —16-fold) and ligands (average —12.1-fold) compared to receptors (average —5.7-fold) and binding proteins (average —4.3-fold) is consistent with known functions of IGF peptides and supports important roles of lncRNAs in prenatal development. Pronounced overall reduction in postnatal expression of IGF system components in lung (—12.9-fold) and kidney (—13.2-fold) are signatures of major changes in organ function while more similar hepatic expression levels (—2.2-fold) are evidence of the endocrine rather than autocrine/paracrine role of IGFs in postnatal growth regulation. Despite its rapid growth, placenta displayed a more stable expression pattern than other organs during prenatal development. Quantitative analyses of contributions of promoters P0-P4 to global *IGF2* transcript in fetal tissues revealed that P4 accounted for the bulk of transcript in all tissues but skeletal muscle. Demonstration of *IGF2* expression in fetal muscle and postnatal liver from a promoter orthologous to mouse and human promoter P0 provides further evidence for an evolutionary and developmental shift

Awards Scholarship provided by the Australian Government. SH is a JS Davies Professorial Fellow. The funders had no role in study design, data collection and analysis, decision to publish, or preparation of the manuscript.

Competing interests: The authors have declared that no competing interests exist.

from placenta-specific P0-expression in rodents and suggests that some aspects of bovine IGF expression may be closer to human than mouse.

Introduction

The insulin-like growth factor (IGF) system is essential for pre- and postnatal growth and development [1–4] and consists of two growth factors (IGF1, IGF2), type 1 and 2 receptors (IGF1R, IGF2R), the insulin receptor (IR) with short and long isoforms (IR-A, IR-B), six major IGF binding proteins (IGFBP1–6) and several lower-affinity binding proteins (IGFBP7 to IGFBP10) [1, 5, 6]. The IGF1 and IGF2 peptides have strong growth promoting endocrine and paracrine/autocrine actions in a wide range of pre- and postnatal tissues and undergo pronounced changes in expression during prenatal development and after birth [7–13]. Consistently, the IGF1 and IGF2 genes have been identified as quantitative trait loci for growth and development in several mammalian species, including mouse, pig, bovine and human [14–25].

Expression of *IGF1* starts early with transcripts detected in preimplantation stage bovine and human embryos and in midgestation rat embryos [26–28]. Transcription of *IGF1* can be initiated from exon 1 or 2, producing *IGF1* class 1 and 2 mRNAs that yield identical mature IGF1 proteins [29–32]. The IGF2 gene is subject to genomic imprinting and paternally expressed in prenatal mammalian tissues, but switches to biallelic expression in a promoter- and tissue specific manner postnatally [33–38]. Interestingly, in mouse, a sequence in *Igf2* intron 2 encodes for an imprinted miRNA that targets non-imprinted *Igf1* transcripts [39–41]. In sheep, pig, bovine and human, *IGF2* transcripts are expressed from four promoters (*IGF2*-P1-4) in a tissue- and developmental stage specific manner [16, 42–47]. The structure of mouse *Igf2* differs significantly from other mammals and transcripts originate from *Igf2*-P1-P3, which are orthologous to *IGF2*-P2-P4 in species discussed above [48], and an additional placenta-specific promoter (P0). Transcripts equivalent to mouse P0 transcripts have also been identified in human fetal skeletal muscle and several postnatal tissues, including heart, lung, liver, muscle and kidney [49, 50]. Furthermore, in mouse, a previously unknown promoter (Pm) is activated preferentially in mesoderm derived tissues by the expression of antisense *H19* long non-coding RNA (*91H*). This *91H*-mediated *Igf2* activation is counteracted by a large excess of *H19* transcripts [51].

The reciprocally imprinted and maternally expressed long non-coding RNA *H19* is located immediately downstream of *IGF2* and expression of both genes is intrinsically linked through shared control elements such as CTCF binding sites [45, 52–56]. More recent analyses in mouse have shown that *H19* harbors miRNAs, one of which regulates cell proliferation and placental size, most likely by targeting *IGF1R* transcript [57]. Furthermore, correlations between *H19* transcript abundance and bovine fetal skeletal muscle and bone mass suggest that development of other organs may be regulated by *H19* [58, 59].

Both IGF ligands signal through combinations of IGF1R and IR homo- and heterodimers, albeit with different affinities. In bovine and human, alternative splicing of the *IR* transcript produces the two receptor isoforms, IR-A and IR-B, that exclude or include exon 11 [60]. Both form heterodimers with each other and IGF1R [61, 62]. IR-A isoform displays higher affinity for IGF2 than IGF1, while IR-B has a high specificity for insulin [63]. The IGF1 peptide signals through homodimers of IGF1R and heterodimers of IGF1R and IR-A or IR-B, while IGF2 peptide signals through homodimers of IGF1R and IR-A and heterodimers of IGF1R and IR-A or IR-A and IR-B [61, 63–65]. The IGF1R gene is expressed ubiquitously and has a major role in maintenance of tissue growth and development [66, 67]. Mutation or ablation of *IGF1R* leads

to growth retardation and/or growth failure more severe than *IGF1* deletion [68]. In human, but not mouse, lack of functional *IR* leads to severe intrauterine growth retardation [69, 70].

In contrast to IGF1R and IR receptors, multifunctional IGF2R is primarily a regulator of IGF2 bioavailability and acts as a scavenger receptor that internalizes IGF2 and targets it for lysosomal degradation [71]. However, studies on stimulation of human trophoblast cell invasion by IGF2 suggest intrinsic signaling functions for IGF2R in placenta via the MAPK pathway [72]. The IGF2R gene is imprinted and maternally expressed in all investigated species, including bovine, with the exception of human, where imprinting appears to be polymorphic [73–77]. Ablation of *IGF2R* in mouse results in severe fetal overgrowth [78] and association of *IGF2R* alleles with postnatal growth parameters in cow suggests a general role for IGF2R in growth regulation [79]. Imprinted expression of mouse *Igf2r* is controlled by a reciprocally imprinted antisense of *Igf2r* non-protein coding RNA *Airn*; orthologues of *Airn* are also expressed in bovine and human [80–82]. However, data on tissue specific developmentally regulated expression of this RNA is lacking.

The IGFBPs modulate bioavailability of IGFs with affinities up to 50-fold higher than IGF1R [83]. Deletion and overexpression models demonstrated organ-specific and general effects of IGFBPs on growth and development [84–87]. The discovery of low affinity IGFBP-related proteins, including IGFBP7 and IGFBP8, has led to the proposal of an IGFBP superfamily [5, 83, 88]. Mice deficient in IGFBP8 die in the perinatal period due to respiratory failure and displayed generalized chondrodysplasia [89].

Expression patterns of genes in the IGF system are highly developmentally regulated [13, 90–100], but changes in tissue specific expression across pre- and postnatal stages by quantitative PCR have not been systematically examined in any species. Here we comprehensively characterize changes in transcript abundances of IGF system genes and associated regulatory long non-coding RNAs in a range of tissues at key developmental time points, i.e., (i) transition from embryo to fetal stage, (ii) fetal stage entering accelerated growth phase and (iii) juvenile stage around puberty. The resulting atlas of tissue- and developmental stage specific expression of the insulin-like growth factor system in bovine is a valuable resource that provides important reference data for future studies of the mammalian IGF system and yields novel insights into similarities and differences between animal model and human.

Materials and methods

Animals and tissues

All animal experiments and procedures described in this study were approved by the University of Adelaide, Adelaide, Australia, Animal Ethics Committee (No. S-094-2005 and S-094-2005A) and the Department of Agriculture, Fisheries and Forestry (DAFF) Animal Ethics Committee, Queensland, Australia (No. SA 2008/01/227 and SA 2010/12/339). We used dams and sires of the two subspecies of domestic cow, *Bos taurus taurus* (Angus, A) and *Bos taurus indicus* (Brahman, B), to generate a large number of purebred and reciprocal cross Day 48 embryos (n = 60) and Day 153 fetuses (n = 73) for samples of prenatal tissues. A set of Day 278 calves (term, Day 277–291, n = 17) was delivered by cesarean section for near term placental samples and later used to obtain samples from juveniles at 12–14 months of age. Further information on samples for RNA extraction and cDNA synthesis (see below) is provided in [S1 Table](#).

To establish pregnancies for recovery of embryos, fetuses and calves, including placenta, dams were subjected to standard commercial estrous cycle synchronization protocols using Cidriol—Heat Detection and Timed Insemination (HTI) and Cidriol—Timed Insemination (TI) procedures as described previously [101]. All pregnancies were confirmed by ultrasound scanning and embryo, fetal and juvenile tissues obtained after sacrificing animals in an

abattoir. All samples were fixed in RNA-later[®] for 24 hours at 4°C before freezing at -80°C until RNA extraction.

RNA isolation and reverse transcription

All fetal and juvenile tissue samples and cesarean section placental samples were homogenized with ceramic beads (MoBio Laboratories, Carlsbad, CA, USA) using the Precellys[®]24 tissue homogenizer (Bertin Technologies, Saint Quentin Yvelines Cedex, France). Total RNA was extracted using TRI Reagent[®] (Ambion, Life Technologies™, Inc., Carlsbad, CA, USA) according to the [manufacturer's instructions](#). Embryonic tissues were homogenized with ceramic beads (MoBio Laboratories, Carlsbad, CA, USA) and the PowerLyzer™ 24 homogenizer (MoBio Laboratories, Carlsbad, CA, USA). Total RNA from embryonic liver and placenta was isolated with TRI Reagent[®]. Due to small sample size for embryonic brain and heart, AllPrep™ DNA/RNA Micro Kits (Qiagen GmbH, Inc., Hilden, Germany) were used for extraction of nucleic acids. Quantity of RNA was determined by repeated measurements with NanoDrop (ThermoFisher Scientific, Waltham, MA, USA). Quality of RNA was assessed using the Agilent RNA 6000 Nano Kit with a Bioanalyzer 2100 (Agilent Technology Inc., Santa Clara, CA, USA). The mean RNA integrity numbers (RIN) of extracted RNAs from different tissues measured by Bioanalyzer System (Agilent Technologies Inc., Santa Clara, CA, USA) are presented in [S2 Table](#).

Complementary DNA (cDNA) was synthesized from 500 ng DNase I (RQ1-DNase, Promega, Madison, WI, USA) treated RNA of each individual tissue sample using SuperScript™ III First-Strand Synthesis System (Invitrogen, Life Technologies™, Inc., Carlsbad, CA, USA) and random hexamer oligonucleotides following the manufacturer's instructions.

Target transcript amplification strategy and quantitative real time PCR

Transcripts quantified included *IGF1* global transcript and the splice variants *IGF1* class 1 and *IGF1* class 2; *IGF2* global transcript and promoter specific transcripts originating from P0, P1 (two transcripts, P1e2 and P1e3), P2 (two splice variants, P2e4 and P2e5), P3 and P4; *IGF1R* and *IGF2R* transcript, *IR* global transcript and splice variants *IR-A* and *IR-B*; *IGFBP1–8*, as well as *H19* and *AIRN* long noncoding RNA transcripts. Primers were designed to be isoform-specific and span two exons or an exon/intron junction to avoid amplification of genomic DNA sequences. Primer information for all amplicons of target genes is detailed in [S3 Table](#). Primer design for promoter and splice variant specific *IGF2* transcripts required extensive in silico analyses in order to be able to assess the complex transcript structure of this gene. Sequences and exon/intron structures for these analyses were retrieved from the literature [[16](#), [43](#)], National Center for Biotechnology Information (NCBI) GenBank database (NCBI reference sequence: AC_000186.1; Gene ID: 281240) and Ensembl project database (ENSBTAG00000013066.5). Since transcripts from P0 promoter were not previously identified in bovine, we performed a sequence similarity search using Basic Local Alignment Search Tool [[102](#)] of NCBI, and identified a highly conserved region upstream of bovine *IGF2* exon 2 that corresponded to the human P0 promoter showing (69% homology) [[50](#)]. Therefore we hypothesized the existence of a putative orthologous promoter in bovine. An overview of our identification and quantification strategy for *IGF2* transcripts in the context of the genomic structure of *INS/IGF2* (GenBank accession no. EU518675.1) is presented in [Fig 1](#).

The first part of this study was designed to systematically measure expression of IGF system components across a broad range of developmental stages and tissues. In light of the fundamental problem to identify stable reference genes across tissues of such rapidly changing developmental stages we opted for a cDNA pooling strategy to assess spatial and temporal differences

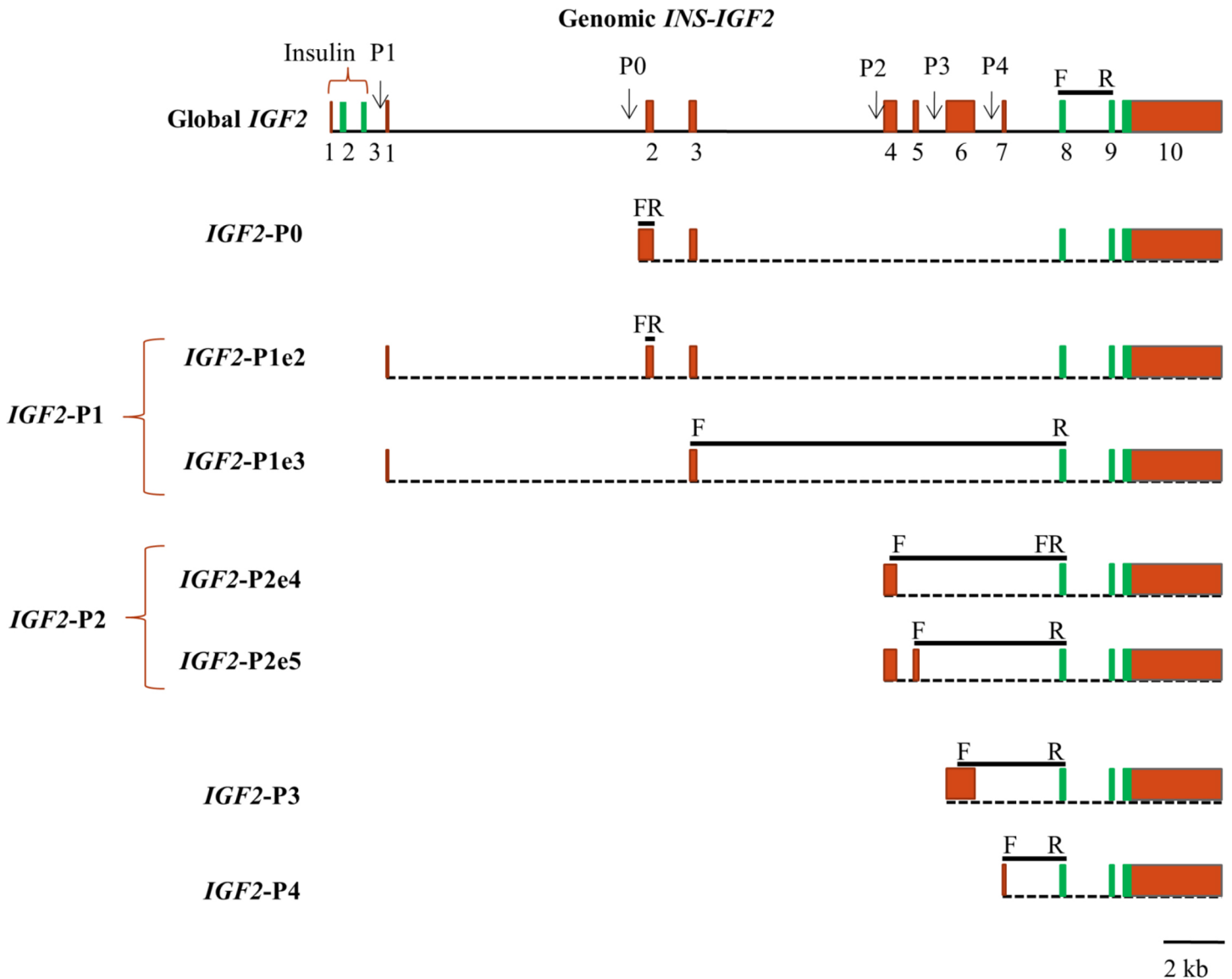


Fig 1. Bovine IGF2 gene and transcript structure with primer locations for amplification of promoter specific transcripts and splice variants. The exon-intron structure of bovine insulin/insulin-like growth factor 2 (*INS/IGF2*, GenBank accession no. EU518675.1) with locations of five promoters (P0, P1, P2, P3 and P4) is shown at the top with promoters (*IGF2-P0 –P4*) and splice variant specific transcripts indicated below. Red and green boxes depict untranslated and protein coding exons, respectively. Forward (F) and reverse (R) primers are indicated with region spanned, including intron where applicable, symbolized by a black bar between primers above the transcript. According to the transcription initiation site of human *IGF2-P0* transcript, the putative orthologous bovine transcript is predicted to originate from a highly conserved region located upstream of the splice donor site of transcript P1 exon 2. We could specifically amplify bovine *IGF2-P0* using a strategically designed forward primer within this unique 5'-UTR sequence and the reverse primer located within exon 2. The two splice variants of P1 promoter transcripts include leading exon 1 which is alternatively spliced onto exons 2 and 3 (*IGF2-P1e2*) and exon 3 (*IGF2-P1e3*) plus the coding exons. In order to amplify the P1 promoter transcripts, two pairs of primers located within exon 2 (for *IGF2-P1e2*) and exons 3 and 8 (for *IGF2-P1e3*) were used. This approach was necessary because specific amplification of transcripts derived from P1 promoter failed due to lack of suitable PCR primer sequence in exon 1. Since *IGF2*-transcript P1 exon 2 is part of the first exonic region of transcript *IGF2-P0*, and exon 3 is present in both *IGF2-P0* and *IGF2-P1* transcripts, the *IGF2-P1e2* and *-P1e3* amplicons could potentially derive from P0 and/or P1 promoters, depending on tissue and developmental stage. We quantified transcript abundances for two splice variants derived from *IGF2-P2* promoter which comprise leading exon 4 (*IGF2-P2e4*) or leading exons 4 and 5 (*IGF2-P2e5*) as well as the protein coding exons. The forward primer for *IGF2-P2e4* was designed to span the junction of exons 4 and 8, and for *IGF2-P2e5* was in exon 5 with the reverse primer for both splice variants in exon 8. To amplify *IGF2-P3* and *IGF2-P4* transcripts, forward primers were designed within exons 6 and 7 with the reverse primer located within exon 8. All primers are detailed in [S3 Table](#).

<https://doi.org/10.1371/journal.pone.0200466.g001>

in expression level. An equal proportion of cDNA from each individual was combined and pooled cDNA used as template in real-time qPCR reactions. The number and sex of individual

tissue cDNA samples from different developmental stages used in cDNA pools is summarized in [S1 Table](#). An equal proportion of cDNA from all tissue- and developmental stage specific cDNA pools was again pooled to generate a cDNA template for standard curve analysis. The standard curve included 3-fold serial dilutions of initial pooled cDNA template over eight data points. Three replicates were used for each dilution of the cDNA template. Real-time qPCR reactions were performed using Fast Start Universal SYBR Green Master (Roche Diagnostics GmbH, Mannheim, Germany) in an Eppendorf Mastercycler[®] ep realplex Real-time PCR System (Eppendorf Inc., Hamburg, Germany) following minimum information for publication of quantitative real-time PCR experiments (MIQE) guidelines [103]. The CT (threshold cycle) values of the standards were used to derive a standard curve which shows the CT values as a linear function of natural logarithm of the specified amounts of cDNA. All qPCR reactions were performed in a total volume of 12 μ l, containing 6 μ l of SYBR master mix, 4 μ l of cDNA (equivalent to 12.5 ng of starting RNA), 0.8 μ l of primers (5 pmol/ μ l) and 1.2 μ l of double distilled nuclease-free water. PCR was carried out with a 10 minute initial denaturation/activation step at 95°C, followed by 40 cycles of 95°C for 20 seconds, 57–62°C (annealing temperatures, [S2 Table](#)) for 30 seconds and 72°C for 20 seconds. Tissue- and developmental stage specific qPCR reactions were performed in triplicate and all investigated tissues and developmental stages were covered in one 96 well plate for each target transcript. Target specificity and integrity was confirmed via sequencing of selected amplicons on a 3730xl DNA Analyzer (Applied Biosystems, Inc., Foster City, CA, USA), plots of the melting curve derived by Mastercycler[®] ep Realplex software (Eppendorf, Inc., Hamburg, Germany), and by electrophoresis of PCR products on a 2% agarose gel (Agarose low EEO, AppliChem GmbH, Darmstadt, Germany) and visual inspection under UV with Gel Doc[™] 1000 Single Wavelength Mini-Transilluminator, using Quantity One image analyzing software (Bio-Rad Laboratories, Inc., Hercules, CA, USA) after staining with GelRed[™] Nucleic Acid Stain (Biotium, Inc., Hayward, CA, USA). Melt-curve dissociation analyses were performed to ensure that amplifications were free of primer dimers; amplification efficiencies were ≥ 0.9 .

The relative abundance of each target transcript was calculated by the relative standard curve method, with determination of PCR amplification efficiency, and expressed in relative units. Transcript abundances are presented in logarithmic scale due to the magnitude of differences between tissues and developmental stages. Since pooled cDNA was used in the quantitative real time RT-PCR reactions for this part of the study, expression data was not normalized using reference genes. We deemed it not appropriate to perform statistical significance tests on technical replicates to compare the average transcript abundances between developmental stages. Rather, we present means and their respective standard deviations from triplicate analyses. Indeed, magnitudes of the vast majority of differences in transcript abundances are such that any statistical testing would have added no meaningful additional information.

Contribution of *IGF2* promoter specific transcripts to global *IGF2* transcript

In the second part of this study we quantified transcript abundances of *IGF2* global and promoter specific transcripts in individual RNA samples of Day 153 fetuses for each of the studied tissues and using Johnson's Relative Weight procedure determined the contribution of the promoter specific transcripts to global expression [104, 105]. This procedure is based on using individual sample values. It requires normalization against reference genes and provides robust estimates for relative promoter-specific contributions to global transcript, including confidence intervals. Each qPCR experiment for this analysis was performed in duplicate and the mean of both CTs used to calculate the amount of target transcript. An equal proportion of cDNA from

all fetuses in each tissue was pooled to generate a cDNA template for standard curve analysis. The standard curve included 2-fold serial dilutions of pooled cDNA template over eight data points, analyzed in triplicate. The relative abundance of each target transcript was automatically calculated by Mastercycler[®] ep Realplex software (Eppendorf, Inc., Hamburg, Germany) using the relative standard curve method.

We determined expression levels of seven putative reference genes identified by a literature search, including actin beta (*ACTB*), ribosomal protein S9 (*RPS9*), ubiquitin B (*UBB*), H3 histone family 3A (*H3F3A*), TATA box binding protein (*TBP*) and vacuolar protein sorting 4 homolog A (*VPS4A*), in each fetal tissue. In placenta, expression level of glyceraldehyde-3-phosphate dehydrogenase (*GAPDH*) was determined instead of *H3F3A*. Details of primers for amplification of reference genes are given in [S4 Table](#). As the variation in expression of reference genes frequently differs between tissues, we used NormFinder [106] to identify the most stably expressed genes in each tissue for normalization following recommended procedures. NormFinder uses a model-based approach which enables ranking of reference genes based on stability values, suggesting the best combination of most stably expressed genes. Tissue-specific stability values for all putative reference genes are summarized in [S5 Table](#). Expression levels of *IGF2* global and promoter specific transcripts in each tissue were normalized to the geometric mean of the expression levels of identified reference genes [107].

The relative contribution of each promoter specific transcript to global *IGF2* transcript abundance was then calculated by Johnson's Relative Weight procedure [104, 105] using an SPSS program developed previously [108]. The following linear regression models were used to analyze tissue-specific relative contributions of promoter specific transcripts (P0, P2, P3 and P4) to global *IGF2* expression:

$$IGF2 \text{ skeletal muscle} = IGF2\text{-P0} + IGF2\text{-P2e4} + IGF2\text{-P2e5} + IGF2\text{-P3} + IGF2\text{-P4}$$

$$IGF2 \text{ liver} = IGF2\text{-P2e4} + IGF2\text{-P2e5} + IGF2\text{-P3} + IGF2\text{-P4}$$

$$IGF2 \text{ placenta,heart,lung,kidney} = IGF2\text{-P2e5} + IGF2\text{-P3} + IGF2\text{-P4}$$

where *IGF2* is the relative expression normalized to the reference genes of global *IGF2*, and *IGF2*-P0, *IGF2*-P3 and *IGF2*-P4 are relative expression of the transcripts derived from P0, P3 and P4 promoters, respectively. *IGF2*-P2e4 (transcript with untranslated leader exon 4) and *IGF2*-P2e5 (transcript with untranslated leader exons 4 and 5) are relative expression of the splice variants derived from P2 promoter. Not every equation includes all promoters due to tissue-specific expression.

Results

Tissue- and developmental stage specific expression of IGF system components

Insulin-like growth factors 1 and 2. Across tissues and developmental stages juvenile liver and fetal skeletal muscle displayed the highest levels of global *IGF1* transcript. Expression in brain and heart peaked at the fetal stage and was lower in most juvenile tissues, with a notable 60.7-fold reduction in lung ([Fig 2](#) and [S6](#) and [S7 Tables](#)). An exception was juvenile liver, where *IGF1* expression was 36.5-fold higher than in fetal liver ([Fig 2](#) and [S7 Table](#)). Generally, across tissues and developmental stages, the pattern of *IGF1* class 1 expression was similar to global *IGF1* expression, while *IGF1* class 2 showed a very different pattern. In addition, postnatal increase in liver *IGF1* class 1 and class 2 transcript differed significantly at 13-fold and 165-fold, respectively ([Fig 2](#)). The highest level of *IGF1* class 2 transcript amongst all prenatal tissues was measured in embryonic placenta, from where it declined towards term ([Fig 2](#)).

Global *IGF2* transcript levels were highest in embryonic and fetal liver, and fetal lung and skeletal muscle, while liver was the major tissue expressing *IGF2* in juveniles. Brain displayed

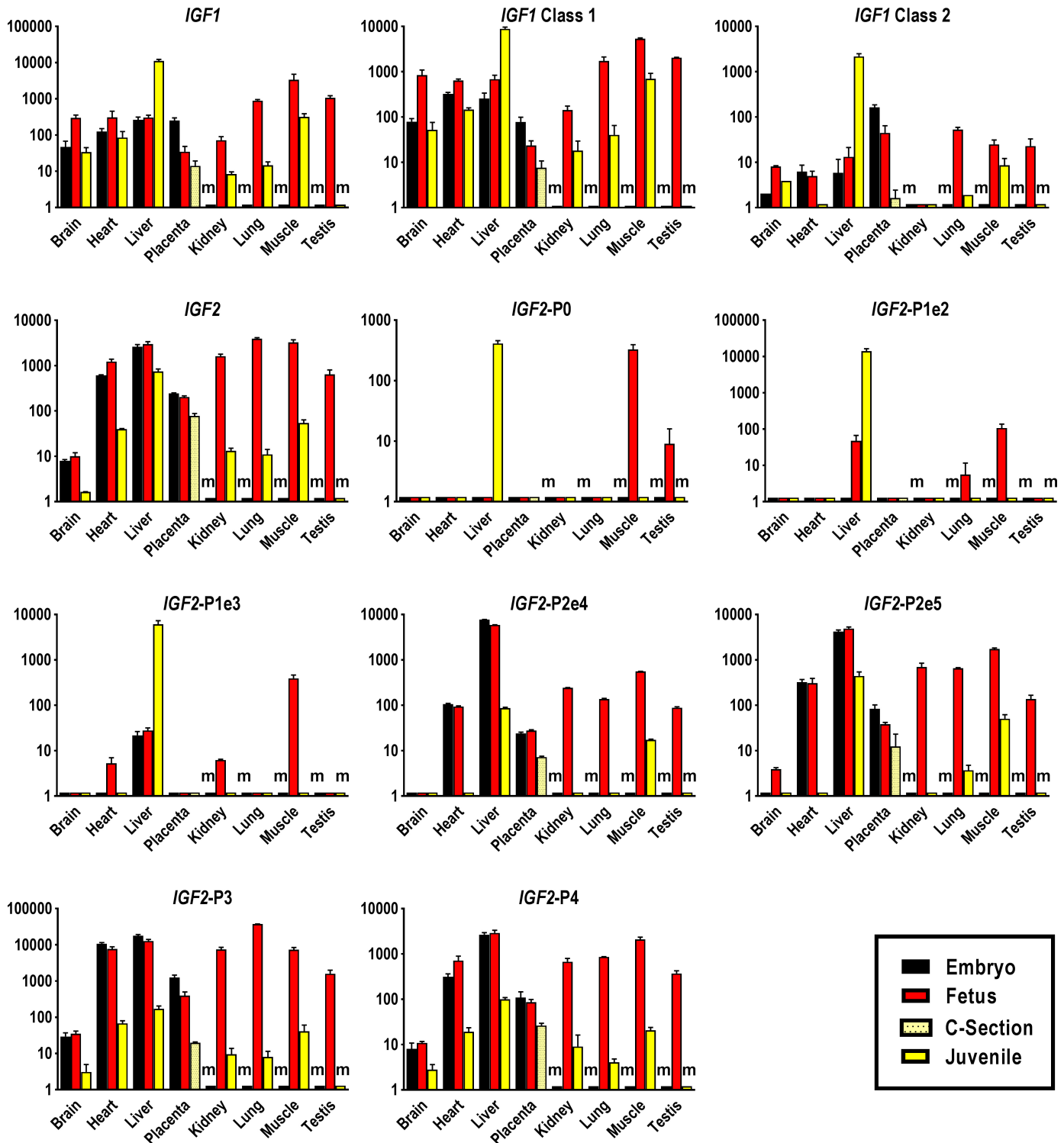


Fig 2. Tissue-specific expression profiles of IGF system ligands in bovine pre- and postnatal developmental stages. Abundances of global *IGF1* transcript and splice variants *IGF1* class 1 and 2, global *IGF2* transcript and promoter and splice variant-specific *IGF2*-P0, *IGF2*-P1e2, *IGF2*-P1e3, *IGF2*-P2e4, *IGF2*-P2e5, *IGF2*-P3 and *IGF2*-P4 transcript were measured in tissues of Day 48 embryos, Day 153 fetuses and 12–14 month-old juveniles. Placental samples were obtained from Day 48 embryos, Day 153 fetuses and term calves born by Caesarean section (C-section) at Day 277/278 of gestation. Means and standard deviations of means for each transcript and tissue were calculated based on triplicate measures of pooled cDNA comprising up to 60 embryonic cDNA samples, 73 fetal cDNA samples, 5 placental cDNA samples of C-section calves and 17 juvenile cDNA samples. Transcript abundances were calculated by the standard curve method and expressed in relative units, and are presented in logarithmic scale. 'm' denotes missing tissue such as kidney that is not yet present in embryos, where transcript abundances could not be determined.

<https://doi.org/10.1371/journal.pone.0200466.g002>

the lowest expression levels of global *IGF2* transcript across all tissues and developmental stages but expression was still subject to substantial developmental change and 6-fold lower in juveniles as compared to prenatal stages (Fig 2 and S6 and S7 Tables). A drastic decline in global *IGF2* expression was evident in juvenile lung where transcript abundance was 355-fold lower as compared to the fetal stage. In contrast, *IGF2* expression in juvenile liver was only 4-fold lower than in fetal liver (Fig 2 and S7 Table).

Prenatal expression of transcripts from *IGF2*-P0 promoter was confined to fetal skeletal muscle and testis, with a 30-fold higher abundance in skeletal muscle. Postnatally, the *IGF2*-P0 transcript was only present in liver and at a level comparable to fetal skeletal muscle (Fig 2). The *IGF2*-P1e2 amplicon was not detected in embryo tissues, but present in fetal skeletal muscle, lung and liver. In juveniles, it was restricted to liver with 294-fold higher abundance than in the fetus. In the embryo, *IGF2*-P1e3 amplicon was only detected in liver, but by the fetal stage it was also present in heart, kidney and, at the highest level of all prenatal tissues, skeletal muscle. In juveniles this amplicon was again restricted to liver at a level 218-fold higher than at the fetal stage (Fig 2).

Comparison of expression patterns of *IGF2*-P2 splice variants revealed that *IGF2*-P2e4 expression was highest in embryonic and fetal liver and 68-fold lower in the juvenile organ. Transcript abundances for *IGF2*-P2e5 followed a similar pattern as *IGF2*-P2e4 except for lung, where it was also detected in juveniles, and for placenta, where it declined from embryo to term (Fig 2).

Expression of *IGF2*-P3 promoter transcript was higher in embryonic heart and liver than at the fetal stage. Apart from brain, where expression across developmental stages was very low, this transcript was subject to striking developmental changes. In juveniles, compared to the fetal stage, expression was reduced by 4639-fold in lung, 775-fold in kidney, 179-fold in skeletal muscle, 113-fold in heart and 74-fold in liver. In placenta, expression of *IGF2*-P3 declined throughout gestation with a 20-fold reduction from fetal stage to term (Fig 2). The developmental and tissue specific expression pattern of *IGF2*-P4 was similar to *IGF2*-P3 except for fetal lung, where *IGF2*-P4 transcript was expressed at the same level as fetal kidney; both *IGF2*-P3 and *IGF2*-P4 expression patterns were more similar to that of global *IGF2* transcript than any other *IGF2* promoter specific transcript (Fig 2).

Insulin-like growth factor receptors 1 and 2 and insulin receptor. In comparison to other receptors, *IR* displayed less variation in expression across tissues and developmental stages (Fig 3 and S6–S8 Tables). The highest global *IR* transcript levels of all embryonic and postnatal tissues were measured in liver while expression at the fetal stage was highest in skeletal muscle and at similar high levels in heart, kidney, liver, lung and testis. Reduction in postnatal *IR* expression was modest with 3.7-, 2.8- and 1.5-fold lower global transcript levels in juvenile kidney, lung and skeletal muscle than in respective fetal tissues. In placenta, global *IR* transcript abundance remained constant from embryo until term (Fig 3 and S6–S8 Tables). The relative temporal-spatial expression pattern for *IR*-A transcript was strikingly similar to global *IR* (Fig 3). As compared to the fetal stage, expression of *IR*-A was 2-fold lower in juvenile brain, heart and liver, and 4- and 3-fold lower in postnatal kidney and lung, respectively (Fig 3). The *IR*-B transcript displayed a somewhat stronger postnatal decline with 2-, 4-, 6- and 9-fold lower transcript levels in juvenile heart, brain, lung, and kidney, respectively than in fetal tissues. In placenta, *IR*-A and *IR*-B transcript levels were remarkably stable throughout gestation (Fig 3).

In brain and liver, *IGF1R* was expressed at similar levels and declined from embryo- to fetal- and juvenile stage. Expression in heart peaked at the fetal stage. In juvenile lung and kidney, transcript levels were 17- and 20-fold lower, respectively, as compared to fetal organs. The highest transcript abundance of *IGF1R* for juveniles was measured in heart and skeletal muscle

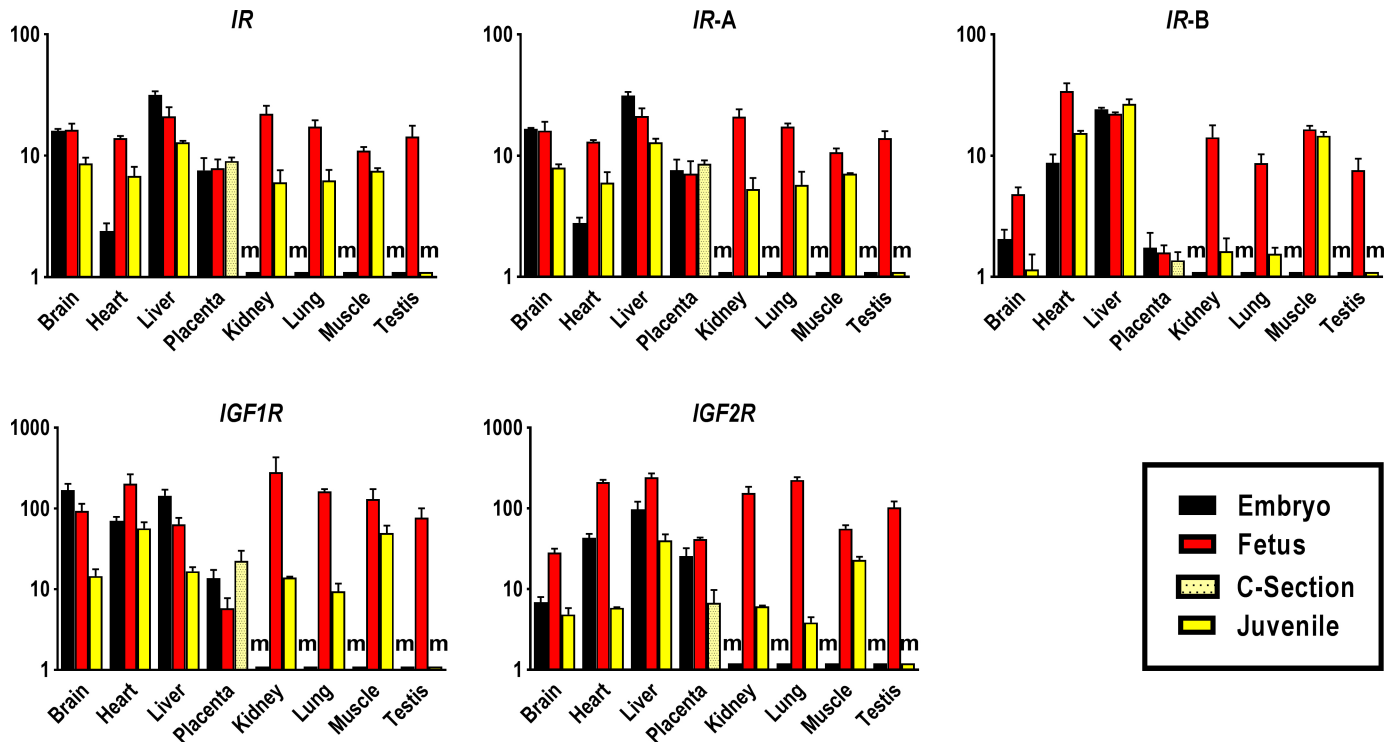


Fig 3. Tissue-specific expression profiles of IGF system receptors in bovine pre- and postnatal developmental stages. Abundances of global *IR* transcript and splice variants *IR-A* and *IR-B*, *IGF1R* and *IGF2R* were measured in tissues of Day 48 embryos, Day 153 fetuses and 12–14 month-old juveniles. Placental samples were obtained from Day 48 embryos, Day 153 fetuses and term calves born by Caesarean section (C-section) at Day 277/278 of gestation. Means and standard deviations of means for each transcript and tissue were calculated based on triplicate measures of pooled cDNA comprising up to 60 embryonic cDNA samples, 73 fetal cDNA samples, 5 placental cDNA samples of C-section calves and 17 juvenile cDNA samples. Transcript abundances were calculated by the standard curve method and expressed in relative units, and are presented in logarithmic scale. ‘m’ denotes missing tissue such as kidney that is not yet present in embryos, where transcript abundances could not be determined.

<https://doi.org/10.1371/journal.pone.0200466.g003>

(Fig 3 and S7 Table). Compared to other prenatal tissues, *IGF1R* transcript was less abundant in placenta, where it was lowest at the fetal stage and highest at term (Fig 3).

Expression of *IGF2R* transcript was highest in fetuses and lowest in juveniles in all investigated tissues. The increase in expression from embryo to fetal stage ranged from 2.5-fold in liver to 4.9-fold in heart with highest transcript levels observed in fetal heart, liver and lung and lowest levels in brain (Fig 3 and S6 Table). In juveniles, *IGF2R* expression was highest in liver followed by skeletal muscle. Lung revealed the most remarkable postnatal change with a 58.6-fold lower transcript level in juvenile compared to the fetal stage. In contrast, postnatal expression of *IGF2R* in skeletal muscle was only 2.4-fold lower than at the fetal stage (Fig 3 and S7 Table). In placenta, *IGF2R* transcript abundance was 6.2-fold lower at term than at mid-gestation (Fig 3 and S8 Table).

Insulin-like growth factor binding proteins. We analyzed expression patterns of high affinity *IGFBP1* to 6 as well as low affinity *IGFBP7* and *IGFBP8* (Fig 4). The *IGFBP1* gene displayed a unique expression pattern among *IGFBPs* with almost exclusive expression in liver at all studied developmental stages where transcript abundance in juvenile was 2-fold lower as compared to prenatal stages (Fig 4, S6 and S7 Tables). At the embryo stage, *IGFBP2* expression was highest in brain with a 14-fold lower transcript abundance by the fetal stage and only a slight further decline in juvenile (Fig 4, S6 and S7 Tables). By the fetal stage, and amongst all sampled tissues, the highest amount of *IGFBP2* transcript was measured in liver. High expression was also detected in kidney, while the lowest amounts of *IGFBP2* transcript were observed

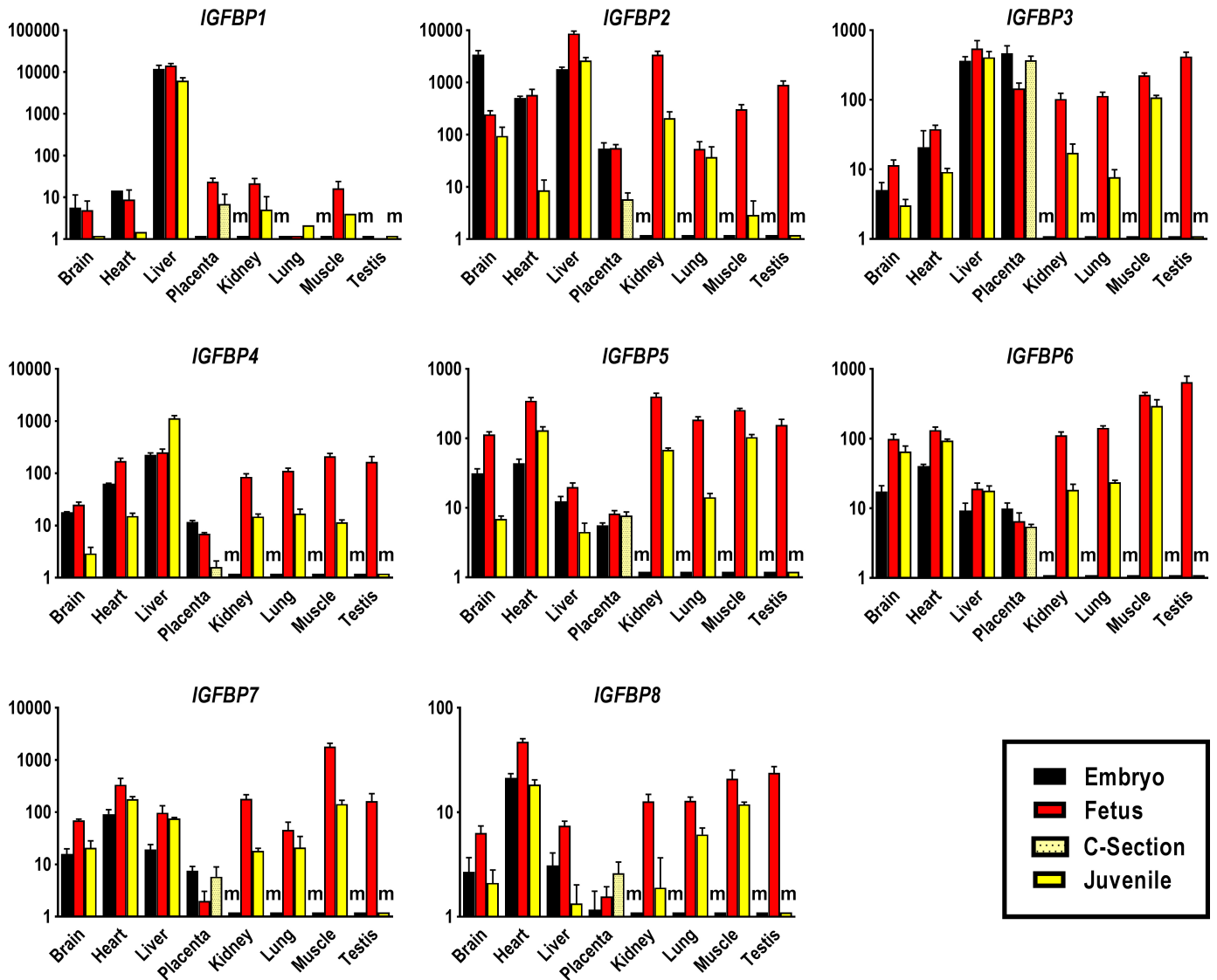


Fig 4. Tissue-specific expression profiles of IGF system binding proteins in bovine pre- and postnatal developmental stages. Abundances of transcripts for *IGFBP1*, *IGFBP2*, *IGFBP3*, *IGFBP4*, *IGFBP5*, *IGFBP6*, *IGFBP7* and *IGFBP8* were measured in tissues of Day 48 embryos, Day 153 fetuses and 12–14 month-old juveniles. Placental samples were obtained from Day 48 embryos, Day 153 fetuses and term calves born by Caesarean section (C-section) at Day 277/278 of gestation. Means and standard deviations of means for each transcript and tissue were calculated based on triplicate measures of pooled cDNA comprising up to 60 embryonic cDNA samples, 73 fetal cDNA samples, 5 placental cDNA samples of C-section calves and 17 juvenile cDNA samples. Transcript abundances were calculated by the standard curve method and expressed in relative units, and are presented in logarithmic scale. ‘m’ denotes missing tissue such as kidney that is not yet present in embryos, where transcript abundances could not be determined.

<https://doi.org/10.1371/journal.pone.0200466.g004>

in fetal lung and placenta. In juvenile, *IGFBP2* expression was still highest in liver at a level similar to the embryonic stage, while transcript abundance in kidney, heart and skeletal muscle were 3–16-, 67- and 106-fold lower than at the fetal stage (Fig 4 and S7 Table). Expression of *IGFBP2* was comparatively low and constant in embryonic and fetal placenta, and further declined by 10-fold at term (Fig 4 and S7 Table). Expression of *IGFBP3* was highest in liver, where it remained stable across developmental time points, and in placenta and testis. Expression was lower in heart and brain, with a peak at the fetal stage. The 15-fold decline in postnatal expression of *IGFBP3* in lung was higher than in any other tissue (Fig 4 and S7 Table). The high level of embryonic placental *IGFBP3* expression was also observed at late gestation (Fig 4). The

IGFBP4 gene was the only gene from the *IGFBP* family whose expression showed a postnatal organ-specific increase in expression level. Here, transcript abundance in juvenile liver was 4.5-fold higher than at the fetal stage. In other juvenile tissues, transcript abundances were lower than at the fetal stage and at a similar level with a more pronounced 18-fold reduction in skeletal muscle. Brain and placenta exhibited the lowest *IGFBP4* transcript levels at all developmental stages (Fig 4 and S7 Table). Expression of *IGFBP5* peaked at the fetal stage in brain, heart and liver and declined in juvenile tissues. The highest transcript levels of *IGFBP5* were measured in fetal heart and kidney. Brain and lung showed the strongest postnatal decline by 16.4- and 13-fold, respectively. In juveniles, *IGFBP5* transcript abundance was highest in heart and skeletal muscle and lowest in brain and liver (Fig 4 and S7 Table). Placenta displayed comparatively low and stable expression levels of *IGFBP5* from embryo to term (Fig 4). Abundance of *IGFBP6* transcript increased from embryo to fetal stage and was highest in fetal testis and skeletal muscle. Expression remained high in juvenile skeletal muscle and only kidney and lung displayed a 6-fold decline in transcript abundance compared to the fetal stage. Similar to *IGFBP5*, expression of *IGFBP6* was lowest in liver and placenta, but unlike *IGFBP5*, expression did not decline markedly in postnatal brain and liver (Fig 4 and S7 Table).

We measured transcript abundances for two low affinity IGFBPs, *IGFBP7* and 8. Expression of *IGFBP7* was highest in skeletal muscle and heart and lowest in placenta at all developmental stages. At the fetal stage, transcript abundance in skeletal muscle was substantially higher than in other tissues followed by a 12.7-fold decline in juvenile skeletal muscle. Postnatal expression of *IGFBP7* in kidney also declined by 10-fold (Fig 4 and S7 Table). Abundance of *IGFBP8* transcripts was highest in heart and lowest in placenta at all developmental stages. Fetal and juvenile skeletal muscle and fetal testis also showed high levels of *IGFBP8* expression. Expression of *IGFBP8* in juvenile tissues was lower with an approximately 6-fold decline in liver and kidney from the fetal stage (Fig 4 and S7 Table).

Tissue- and developmental stage specific expression of lncRNAs

We investigated expression of the two imprinted long non-coding RNA genes associated with the IGF system, *H19* and *AIRN*. Across all tissues, expression of *H19* was highest in the embryo, declined slightly by the fetal stage and was substantially lower in juvenile (Fig 5, S6 and S7 Tables). Embryonic and fetal liver displayed the highest, and brain the lowest, *H19* transcript levels of all prenatal tissues. Similar and comparatively high levels of *H19* transcript were found in fetal kidney, lung and skeletal muscle with somewhat lower levels in heart and testis. Kidney displayed the strongest decline in postnatal *H19* expression with more than 100-fold lower transcript abundance as compared to the fetal stage. Amongst postnatal tissues, *H19* transcript level was highest in skeletal muscle which displayed a 9-fold reduction from fetal to juvenile stage. Expression of *H19* in placenta declined 2-fold from embryo to fetal stage and was unchanged at term (Fig 5, S7 and S8 Tables).

Expression of *AIRN* transcript increased from embryo to fetal stage and declined in juvenile tissues (Fig 5, S6 and S7 Tables). Across developmental stages *AIRN* transcript was most abundant in liver with 10-fold lower expression in juvenile. Expression was also high in fetal kidney and lung, which showed the strongest decline in transcript abundance with 58- and 29-fold lower transcript levels in juvenile. Brain and heart displayed similar *AIRN* expression levels at the embryo and juvenile stages and brain, heart and skeletal muscle had a similar, milder reduction in expression level in juvenile as compared to fetal tissues (Fig 5, S7 Table). Placental expression of *AIRN* was similar at the embryo and fetal stage, but 6-fold lower at term (Fig 5 and S8 Table).

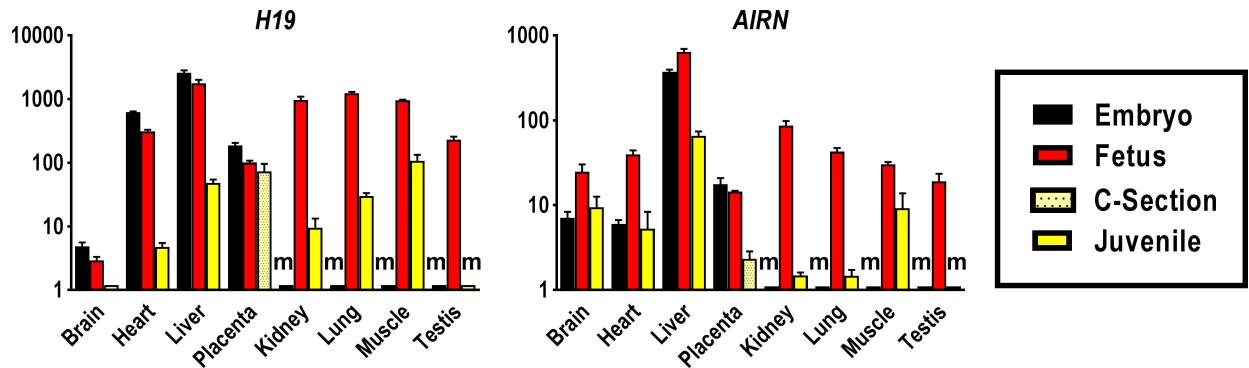


Fig 5. Tissue-specific expression profiles of long non-coding RNAs associated with the IGF system in bovine pre- and postnatal developmental stages. Abundances of *H19* and *AIRN* transcript were measured in tissues of Day 48 embryos, Day 153 fetuses and 12–14 month-old juveniles. Placental samples were obtained from Day 48 embryos, Day 153 fetuses and term calves born by Caesarean section (C-section) at Day 277/278 of gestation. Means and standard deviations of means for each transcript and tissue were calculated based on triplicate measures of pooled cDNA comprising up to 60 embryonic cDNA samples, 73 fetal cDNA samples, 5 placental cDNA samples of C-section calves and 17 juvenile cDNA samples. Transcript abundances were calculated by the standard curve method and expressed in relative units, and are presented in logarithmic scale. ‘m’ denotes missing tissue such as kidney that is not yet present in embryos, where transcript abundances could not be determined.

<https://doi.org/10.1371/journal.pone.0200466.g005>

Contribution of promoter specific *IGF2* transcripts to global *IGF2* transcript abundance in fetal tissues

We determined for the first time the contribution of promoter-specific *IGF2* transcripts (Figs 1 and 2) to global *IGF2* transcript in fetal tissues including placenta by multiple regression analysis (Fig 6). Estimated means with 95% confidence intervals are presented in S9 Table. Contributions of 53%, 61%, 72% and 90% to global *IGF2* transcript identified *IGF2*-P4 as the predominant promoter in bovine fetal liver, lung, heart and kidney, respectively. This promoter was also responsible for 64% of all *IGF2* transcripts measured in placenta. Amongst all tissues studied, *IGF2*-P4 was least active in skeletal muscle but it still contributed 28% of global transcript. The second most abundant transcript in fetal lung, heart and placenta was *IGF2*-P2 derived *IGF2*-P2e5, accounting for 31%, 24%, and 24% of global transcript, respectively. However in fetal liver and skeletal muscle, the alternative splice variant derived from *IGF2*-P2 promoter, *IGF2*-P2e4 transcript, dominated and accounted for 44% and 35% of global *IGF2* expression, respectively. Although *IGF2*-P0 accounted for 30% of global *IGF2* and was therefore one of the most common *IGF2* transcripts in muscle, it did not contribute to *IGF2* expression in any other fetal tissue or placenta. Promotor *IGF2*-P3 was active at low levels with contributions of 1–8% in fetal tissues and 12% in placenta.

Discussion

We provide here an atlas of tissue- and developmental stage specific gene expression for the bovine insulin-like growth factor (IGF) system, including imprinted long non-coding (lnc) RNAs *H19* and *AIRN*. This mammalian IGF expression catalogue informs basic and comparative IGF research and provides reference data for an important agricultural species and biomedical model.

Our comprehensive profile of expression patterns and comparisons of pre- and postnatal changes in expression of IGF ligands support established roles of *IGF1* in growth and development [109]. Across developmental stages and tissues, global *IGF1* expression was highest in juvenile liver, consistent with data from sheep [31, 110], mouse [111] and rat [112–114]. However, *IGF1* expression in all other tissues peaked at the fetal stage, a clear indication of the

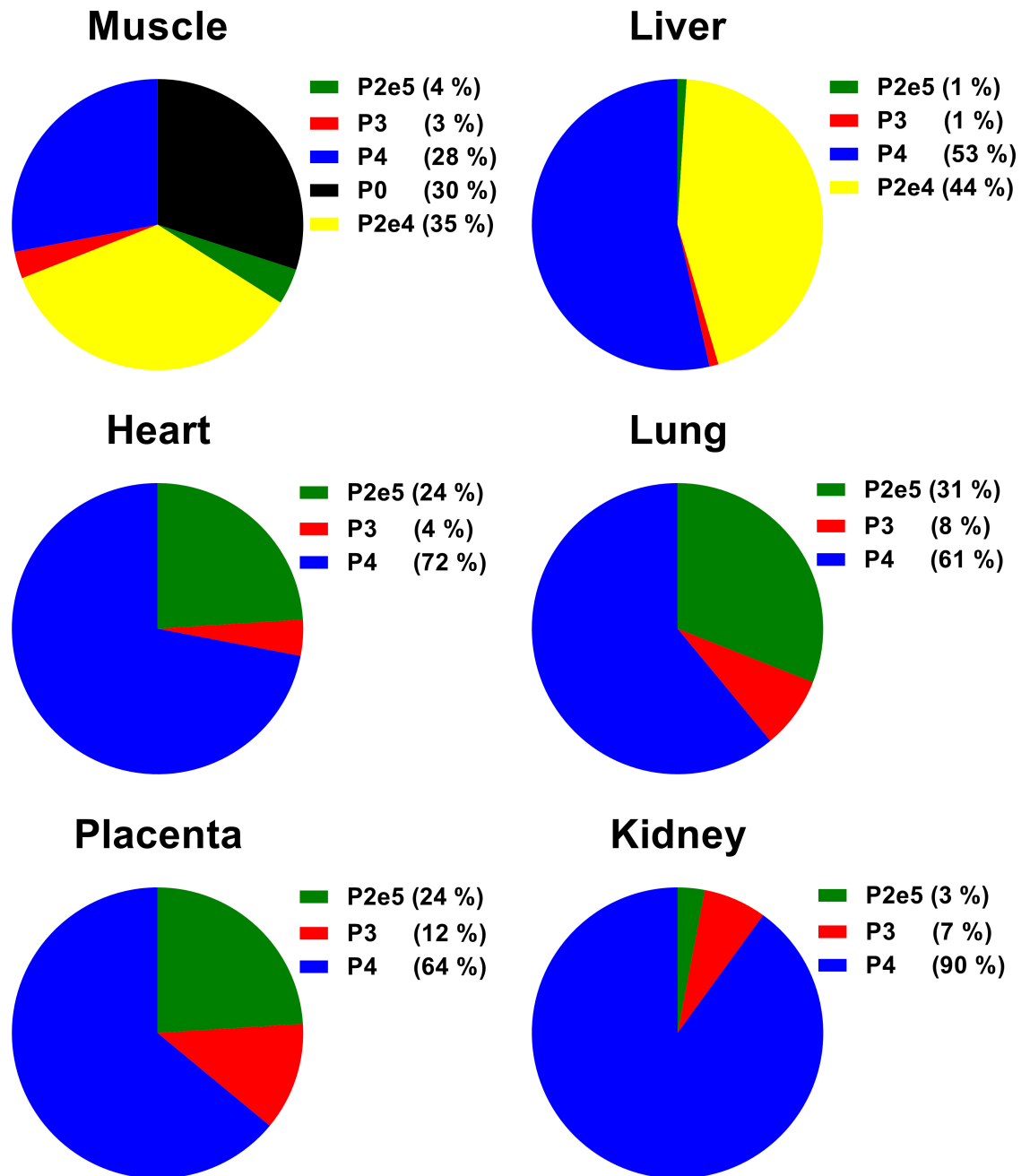


Fig 6. Relative contribution of promoter and splice variant-specific *IGF2* transcripts to global *IGF2* transcript abundance in fetal tissues and placenta. *IGF2*-P0, *IGF2*-P3 and *IGF2*-P4 are percent transcript abundance derived from P0, P3 and P4 promoters, respectively. Splice variants of promoter P2 transcript are *IGF2*-P2e4 with untranslated leader exon 4 and *IGF2*-P2e5 with untranslated leader exons 4 and 5. Estimated means are from 73 fetal cDNA samples per tissue and 95% confidence intervals are detailed in S9 Table. Transcript abundances were calculated by the standard curve method, normalized with reference genes and expressed in relative units. The relative contribution of each promoter-specific transcript to global *IGF2* transcript abundance was calculated by Johnson's Relative Weight procedure.

<https://doi.org/10.1371/journal.pone.0200466.g006>

significant role of IGF1 in mammalian prenatal growth [2, 97, 115, 116]. As reported previously [117], expression was highest in fetal muscle where IGF1 has protein anabolic effects [118]. The expression pattern for *IGF1* class 1 transcript was more similar to *IGF1* global

transcript, suggesting that class 1 is the predominant transcript across tissues and developmental stages. In skeletal muscle and liver of the third trimester sheep fetus, IGF1 class 1 transcript was also much more abundant than class 2 transcript [97]. Expression of IGF1 class 2 transcript displayed considerable developmental stage and tissue specificity, with strongest expression in postnatal liver. Stronger postnatal hepatic expression of IGF1 class 2 compared to class 1 transcript could be due to greater dependency of this transcript on growth hormone as shown in sheep [110]. Our data thus extends previous limited information on IGF1 class 1 and 2 transcript expression in pre- and postnatal tissues of cattle [119, 120], sheep [97, 110, 121], pig [122, 123], mouse [124] and rat [125] to earlier embryo-fetal stages.

We found that expression of IGF2 was broadly similar in embryonic and fetal bovine tissues, but much lower in juvenile tissues. Postnatal decline in expression of global IGF2 transcript was considerably stronger than for IGF1, highlighting the special role of IGF2 in prenatal growth and development described previously [126–128]. Significant downregulation of IGF2 after birth has been reported for cattle, sheep and human [90–92, 98, 129]. In rat, IGF2 transcripts were undetectable by Northern blot in all adult tissues except brain, spinal cord and striated muscle [13, 130, 131]. Postnatal decline in IGF2 expression was least in liver, the major source of circulating IGF2 in adults [8] and consistent with considerable IGF2 levels in adult cattle [132]. The higher expression of IGF2 in postnatal liver compared to other tissues may be caused by tissue-specific relaxation of IGF2 imprinting or a change from imprinted to non-imprinted promoter use as previously demonstrated in human [37, 133]. The exclusive expression of IGF2-P0 transcript in juvenile liver and high levels of IGF2-P1e2 and -P1e3 transcripts in this tissue may reflect a combined imprinted/non-imprinted promoter scenario. In human, P0 transcript is expressed from the paternal allele while P1 transcripts show biallelic expression at all developmental stages [37, 50].

Exclusive expression of IGF2-P0 transcript in bovine fetal skeletal muscle and testis, is in agreement with reported IGF2-P0 expression in human fetal skeletal muscle [50]. To our knowledge fetal testis has not yet been tested for expression of IGF2-P0 transcript in human or any other species. Human and bovine thus indicate an evolutionary shift in IGF2 expression from mouse, where *Igf2*-P0 transcript is confined to placenta [127]. We also demonstrate for the first time a developmental shift in tissue-specificity of IGF2-P0, which is no longer active in juvenile bovine skeletal muscle but active in juvenile liver. This contrasts with ubiquitous IGF2-P0 expression in adult human tissues [50] although some of these differences may be explained by the different developmental age of bovine tissues studied.

Splice variants of IGF2-P1 transcripts including exon 1, which is alternatively spliced onto exons 2 and/or 3 as well as the coding exons, were previously observed in bovine [16], pig [44], human [134, 135] and sheep [42]. Considering sequence based restrictions of our IGF2 promoter 1-specific transcript amplification strategy described in Fig 1, and our finding that IGF2-P0 transcript is the predominant transcript in bovine fetal skeletal muscle, IGF2-P1e2 and IGF2-P1e3 transcripts detected in this tissue could potentially originate from the IGF2-P0 promoter. However, we conclude that IGF2-P1e2 and IGF2-P1e3 transcripts in liver, whose abundance increased in postnatal tissue, predominantly derive from IGF2-P1 promoter activity. This is based on an IGF2-P0 expression level in juvenile liver similar to that in fetal skeletal muscle and the fact that relative transcript abundance of IGF2-P1e2 and IGF2-P1e3 in juvenile liver was 130-fold and 15-fold higher than in fetal muscle. Our demonstration of increased activity of IGF2-P1 promoter in postnatal liver where IGF2-P2, IGF2-P3 and IGF2-P4 activity decreases, is consistent with the developmental shift in promoter activity reported for human [46, 50], pig [44], sheep [42, 91] and bovine [92].

Temporal-spatial expression patterns of the two splice variants that originate from IGF2-P2 promoter, IGF2-P2e4 and P2e5, showed some similarities (Fig 2), but quantitative analyses of

promoter-specific transcripts in fetal tissues revealed that only *IGF2-P2e4* variant is a major contributor to *IGF2* transcript abundance in fetal liver and skeletal muscle (Fig 6). This suggests that *IGF2-P2e4* could be actively involved in the production of endocrine IGF2 in the bovine fetus.

Analysis of contributions of promoter specific *IGF2* transcripts to global *IGF2* transcript expression revealed that *IGF2-P3* and *IGF2-P4* are the least and most active promoters, respectively, in all bovine fetal tissues except kidney. This is in agreement with data from fetal mouse and rat, where *IGF2-P3*, which is orthologous to bovine *IGF2-P4* promoter, was most active [48], but differs somewhat from human where *IGF2-P3* and *IGF2-P4*, both orthologues of the respective bovine promoters, were active at high and moderate levels [136].

Amongst receptors studied, relative spatio-temporal expression patterns for global *IR* and splice variant *IR-A* were more stable than those for *IGF1R* and *IGF2R*. This may be explained by predominant involvement of insulin receptors in metabolic pathways, rather than in engineering growth responses [137]. Mice without *Insr* display virtually unimpaired prenatal development with only slight reduction in birth weight [70] and catastrophic loss of metabolic control only after birth [7, 138]. The similarity in expression patterns of *IR* global transcript and *IR-A* suggests that *IR-A* is the predominant isoform of insulin receptor expressed in tissues. The most notable change, and consistent with other relative changes in expression patterns in the IGF system, was the decline in postnatal *IR-B* transcript in kidney and lung.

The similarity in expression patterns of *IGF2R* and *IGF2* is consistent with the crucial role of *IGF2R* for normal development [139]. Observed concomitant downregulation of *IGF2R* and *IGF2* could be expected from the essential regulatory function of *IGF2R* for IGF2 bioavailability [7, 61, 96, 140]. Evidence for active signaling of IGF2 through *IGF2R* has been reported and several lines of evidence suggest that IGF2 stimulates trophoblast migration through *IGF2R* [72, 141, 142]. This is consistent with the stable expression of *IGF2* and *IGF2R* in placenta from embryo to fetal stage and the decline in both transcripts at term in the present study.

Transcript abundances for IGFBPs revealed exclusive strong *IGFBP1* expression in liver across all developmental stages. A similar expression pattern has been reported for fetal liver in mouse and human [143, 144] and fetal and adult liver in rat [145, 146] and reflects the endocrine role of *IGFBP1* [147–150]. The postnatal decrease in expression of *IGFBP2* in skeletal muscle, heart and kidney suggests a significant role before birth. This is supported by higher circulating *IGFBP2* levels in the fetus as compared to adults in a number of species including rat, human, pig and rhesus monkey [99, 151–154]. The relative expression pattern of *IGFBP3* in postnatal tissues showed similarity to the pattern observed for postnatal *IGF1* expression. In the sheep fetus, circulating *IGFBP3* levels are positively correlated with *IGF1* [117, 155]. Expression of *IGFBP3* in placenta remained high throughout gestation. In human and rhesus monkey placenta *IGFBP3* is co-expressed with *IGF2* and has been proposed to modulate IGF2 effects in an autocrine/paracrine fashion [156, 157]. The *IGFBP4* gene stands out as the only binding protein gene that displayed an increase in transcript abundance in a juvenile tissue, i.e., liver. This is consistent with increased *IGFBP4* expression in neonatal pig liver [100] and increased circulating *IGFBP4* in sheep after birth [155]. It is possible that the postnatal increase in hepatic *IGFBP4* expression is associated with increased expression of *IGF1*. It has been demonstrated that *IGFBP4* enhances growth stimulatory effects of endocrine IGF1 by increasing bioavailability of IGF1 via an *IGFBP4* protease-dependent mechanism [158]. High levels of *IGFBP6* expression in fetal and juvenile bovine skeletal muscle may be explained by the involvement of this gene in inhibiting IGF2-induced proliferation and differentiation of myoblasts [159]. Similarly, high level of *IGFBP7* expression in bovine fetal skeletal muscle may also be associated with a potential role in inhibiting myoblast differentiation [160, 161].

The most pronounced changes in transcript levels from pre- to postnatal stages were evident in lncRNAs, consistent with the fundamental roles of this RNA class in growth and development [162–165]. Substantially greater spatio-temporal changes in expression of *H19* as compared to *AIRN* highlights the pivotal functions of *H19* RNA as source of regulatory miRNA that impact *IGF1R* and Smad transcription factors [57, 166] and thus contribute to its role as a major regulator of an imprinted gene network [167] that controls growth [168]. Across tissues and for each developmental stage, relative expression patterns for *H19* were highly similar to those for *IGF2*, which is consistent with current models for coordinated regulation of both genes [169–171]. Cell lineage dependent *H19* expression has been described in sheep [172] and the human fetus [173] where, as in the present study, transcript abundance was lowest in brain. We found that expression of *H19* in bovine fetal kidney, lung and liver was at similar high levels or higher than in fetal skeletal muscle, where it was originally described as a major regulator of prenatal growth and differentiation [168]; whether *H19* has a similar role in these tissues remains to be elucidated. Expression of *H19* in juvenile tissues was much lower than at prenatal stages, except for skeletal muscle, where significant transcription persists. This suggests that growth regulatory functions of *H19* in bovine prenatal muscle [168] may continue well into postnatal development. High levels of *H19* RNA have also been found in postnatal skeletal muscle of mouse, where *H19* encoded miRNAs promote differentiation and regeneration [166].

In light of observed similarities in *H19/IGF2* expression patterns, the different spatio-temporal patterns for *AIRN* and *IGF2R* transcript abundances are somewhat unexpected. Considering the antisense nature of *AIRN/IGF2R* transcripts and their mutually exclusive, interdependent mode of expression in mouse, where *AIRN* RNA silences *IGF2R* [81, 174, 175] an inverse relationship could have been expected. The seemingly unrelated expression patterns may indicate species differences and/or further, possibly organ-specific, roles of *AIRN* in silencing additional imprinted genes [175] or involvement in trans-regulatory processes similar to those identified for *H19* [165].

Lung and kidney showed the highest and liver the lowest relative postnatal reduction in expression of IGF system components. This may be explained by additional prenatal functions of lung and kidney as the flow of fluid from the fetal lung and bladder are major contributors to amniotic fluid [176, 177]. Interestingly, amniotic fluid is a significant source of IGFs [178] as large amounts of fluid are swallowed by the fetus [179] and growth factors cross the gut to enter systemic circulation [180]. The lesser changes in postnatal liver likely reflect the continuing role of this organ as a major source of circulating IGF system components [8, 181–183].

To our knowledge, this is the first comprehensive study in any species to investigate changes in expression of IGF system components and their major regulatory lncRNAs across tissues and developmental stages using real time qPCR. Our expression atlas for the bovine insulin-like growth factor system provides important reference data for future studies of the mammalian IGF system. This includes dissection of prenatal effects on postnatal phenotype where IGF system components and epigenetic mechanisms regulating them, including imprinting and miRNAs, appear to be major programming components [181, 184–187].

Supporting information

S1 Table. Number and sex of individuals used for developmental stage and tissue-specific cDNA pools.

(DOCX)

S2 Table. RNA integrity number (RIN) of RNA extracted from different tissues.

(DOCX)

S3 Table. Details of forward (F) and reverse (R) primers used for amplification of transcripts of target genes.

(DOCX)

S4 Table. Details of forward (F) and reverse (R) primers used for amplification of transcripts of reference genes.

(DOCX)

S5 Table. Stability values for studied reference genes and best combination of genes for different tissues as calculated by NormFinder.

(DOCX)

S6 Table. Comparison of changes in gene expression in the bovine IGF system between Day 48 embryo and Day 153 fetal stages.

(DOCX)

S7 Table. Comparison of changes in gene expression in the bovine IGF system between Day 153 fetal and 12–14 month juvenile stages.

(DOCX)

S8 Table. Comparison of changes in gene expression in the bovine IGF system of placenta from embryo stage to term.

(DOCX)

S9 Table. Estimated relative contributions of *IGF2* promoter-specific transcripts to global *IGF2* transcript abundance with 95% confidence intervals for each fetal tissue.

(DOCX)

Acknowledgments

We are grateful for access to South Australian Research Development Institute research facilities and to Struan Research Centre staff for animal management. We would also like to thank former members of the JS Davies Epigenetics and Genetics Group for their help in sample collection.

Author Contributions

Conceptualization: Karen L. Kind, Stefan Hiendleder.

Data curation: Mani Ghanipoor-Samami, Ali Javadmanesh.

Formal analysis: Mani Ghanipoor-Samami, Ali Javadmanesh, Consuelo Amor S. Estrella, Karen L. Kind.

Funding acquisition: Stefan Hiendleder.

Investigation: Mani Ghanipoor-Samami, Ali Javadmanesh, Brian M. Burns, Dana A. Thomsen, Consuelo Amor S. Estrella, Stefan Hiendleder.

Methodology: Mani Ghanipoor-Samami, Ali Javadmanesh, Greg S. Nattrass, Karen L. Kind, Stefan Hiendleder.

Project administration: Dana A. Thomsen, Stefan Hiendleder.

Resources: Brian M. Burns, Greg S. Nattrass, Stefan Hiendleder.

Supervision: Karen L. Kind, Stefan Hiendleder.

Validation: Mani Ghanipoor-Samami, Ali Javadmanesh, Karen L. Kind, Stefan Hiendleder.

Visualization: Mani Ghanipoor-Samami, Ali Javadmanesh.

Writing – original draft: Mani Ghanipoor-Samami.

Writing – review & editing: Karen L. Kind, Stefan Hiendleder.

References

1. Allan GJ, Flint DJ, Patel K. Insulin-like growth factor axis during embryonic development. *Reproduction*. 2001; 122(1):31–9. PubMed PMID: WOS:000169731400004. PMID: [11425327](#)
2. Woods KA, Camacho-Hübner C, Savage MO, Clark AJL. Intrauterine growth retardation and postnatal growth failure associated with deletion of the insulin-like growth factor I gene. *N Engl J Med*. 1996; 335(18):1363–7. <https://doi.org/10.1056/NEJM199610313351805> PMID: [8857020](#).
3. Lupu F, Terwilliger JD, Lee K, Segre GV, Efstratiadis A. Roles of growth hormone and insulin-like growth factor 1 in mouse postnatal growth. *Dev Biol*. 2001; 229(1):141–62. <https://doi.org/10.1006/dbio.2000.9975>. PMID: [11133160](#)
4. Baker J, Liu J-P, Robertson EJ, Efstratiadis A. Role of insulin-like growth factors in embryonic and postnatal growth. *Cell*. 1993; 75(1):73–82. [https://doi.org/10.1016/s0092-8674\(05\)80085-6](https://doi.org/10.1016/s0092-8674(05)80085-6) PMID: [8402902](#)
5. Kim H-S, Nagalla SR, Oh Y, Wilson E, Roberts CT, Rosenfeld RG. Identification of a family of low-affinity insulin-like growth factor binding proteins (IGFBPs): Characterization of connective tissue growth factor as a member of the IGFBP superfamily. *Proc Natl Acad Sci U S A*. 1997; 94(24):12981–6. PMID: [9371786](#)
6. Denley A, Cosgrove LJ, Booker GW, Wallace JC, Forbes BE. Molecular interactions of the IGF system. *Cytokine Growth Factor Rev*. 2005; 16(4):421–39. <https://doi.org/10.1016/j.cytogfr.2005.04.004>.
7. Nakae J, Kido Y, Accili D. Distinct and overlapping functions of insulin and IGF-I receptors. *Endocr Rev*. 2001; 22(6):818–35. <https://doi.org/10.1210/edrv.22.6.0452> PMID: [11739335](#).
8. O'Dell SD, Day INM. Molecules in focus Insulin-like growth factor II (IGF-II). *Int J Biochem Cell Biol*. 1998; 30(7):767–71. [https://doi.org/10.1016/S1357-2725\(98\)00048-X](https://doi.org/10.1016/S1357-2725(98)00048-X). PMID: [9722981](#)
9. Roith DL, Scavo L, Butler A. What is the role of circulating IGF-I? *Trends Endocrinol Metab*. 2001; 12(2):48–52. [https://doi.org/10.1016/S1043-2760\(00\)00349-0](https://doi.org/10.1016/S1043-2760(00)00349-0). PMID: [11167121](#)
10. Holly JMP, Wass JAH. Insulin-like growth factors; autocrine, paracrine or endocrine? New perspectives of the somatomedin hypothesis in the light of recent developments. *J Endocrinol*. 1989; 122(3):611–8. <https://doi.org/10.1677/joe.0.1220611> PMID: [2478648](#)
11. Klover P, Hennighausen L. Postnatal body growth is dependent on the transcription factors signal transducers and activators of transcription 5a/b in muscle: A role for autocrine/paracrine insulin-Like growth factor I. *Endocrinology*. 2007; 148(4):1489–97. <https://doi.org/10.1210/en.2006-1431> PMID: [17158201](#).
12. Shoba L, An MR, Frank SJ, Lowe Jr WL. Developmental regulation of insulin-like growth factor-I and growth hormone receptor gene expression. *Mol Cell Endocrinol*. 1999; 152(1–2):125–36. [https://doi.org/10.1016/S0303-7207\(99\)00045-3](https://doi.org/10.1016/S0303-7207(99)00045-3). PMID: [10432230](#)
13. Brown AL, Graham DE, Nissley SP, Hill DJ, Strain AJ, Rechler MM. Developmental regulation of insulin-like growth factor II mRNA in different rat tissues. *J Biol Chem*. 1986; 261(28):13144–50. PMID: [3759952](#)
14. Jeon JT, Carlborg O, Tornsten A, Giuffra E, Amarger V, Chardon P, et al. A paternally expressed QTL affecting skeletal and cardiac muscle mass in pigs maps to the *IGF2* locus. *Nat Genet*. 1999; 21(2):157–8. PubMed PMID: ISI:000078399500013. <https://doi.org/10.1038/5938> PMID: [9988263](#)
15. Vykoukalová Z, Knoll A, Dvořák J, Čepica S. New SNPs in the *IGF2* gene and association between this gene and backfat thickness and lean meat content in Large White pigs. *J Anim Breed Genet*. 2006; 123(3):204–7. <https://doi.org/10.1111/j.1439-0388.2006.00580.x> PMID: [16706926](#)
16. Goodall JJ, Schmutz SM. *IGF2* gene characterization and association with rib eye area in beef cattle. *Anim Genet*. 2007; 38(2):154–61. <https://doi.org/10.1111/j.1365-2052.2007.01576.x> PubMed PMID: ISI:000245311300010. PMID: [17403010](#)
17. Heude B, Ong KK, Luben R, Wareham NJ, Sandhu MS. Study of association between common variation in the insulin-like growth factor 2 gene and indices of obesity and body size in middle-aged men and women. *J Clin Endocrinol Metab*. 2007; 92(7):2734–8. <https://doi.org/10.1210/jc.2006-1948> PMID: [17488802](#).

18. Fan B, Onteru SK, Du Z-Q, Garrick DJ, Stalder KJ, Rothschild MF. Genome-wide association study identifies loci for body composition and structural soundness traits in pigs. *PLoS One*. 2011; 6(2). <https://doi.org/10.1371/journal.pone.0014726> PubMed PMID: WOS:000287761700004. PMID: 21383979
19. Van Laere AS, Nguyen M, Braunschweig M, Nezer C, Collette C, Moreau L, et al. A regulatory mutation in *IGF2* causes a major QTL effect on muscle growth in the pig. *Nature*. 2003; 425(6960):832–6. <https://doi.org/10.1038/nature02064> PubMed PMID: ISI:000186118500044. PMID: 14574411
20. Sutter NB, Bustamante CD, Chase K, Gray MM, Zhao K, Zhu L, et al. A single *IGF1* allele is a major determinant of small size in dogs. *Science*. 2007; 316(5821):112–5. <https://doi.org/10.1126/science.1137045> PMID: 17412960
21. Rosen CJ, Churchill GA, Donahue LR, Shultz KL, Burgess JK, Powell DR, et al. Mapping quantitative trait loci for serum insulin-like growth factor-1 levels in mice. *Bone*. 2000; 27(4):521–8. [https://doi.org/10.1016/S8756-3282\(00\)00354-9](https://doi.org/10.1016/S8756-3282(00)00354-9). PMID: 11033447
22. Zhao Q, Davis ME, Hines HC. Associations of an *Acil* polymorphism in the IGF-II gene with growth traits in beef cattle. 7th World Congress on Genetics Applied to Livestock Production; Montpellier, France2002.
23. Zwierzchowski L, Siadkowska E, Oprzadek J, Flisikowski K, Dymnicki E. An association of C/T polymorphism in exon 2 of the bovine insulin-like growth factor 2 gene with meat production traits in Polish Holstein-Friesian cattle. *Czech J Anim Sci*. 2010; 55(6):227–33. PubMed PMID: WOS:000279340300002.
24. Sherman EL, Nkrumah JD, Murdoch BM, Li C, Wang Z, Fu A, et al. Polymorphisms and haplotypes in the bovine neuropeptide Y, growth hormone receptor, ghrelin, insulin-like growth factor 2, and uncoupling proteins 2 and 3 genes and their associations with measures of growth, performance, feed efficiency, and carcass merit in beef cattle. *J Anim Sci*. 2008; 86(1):1–16. <https://doi.org/10.2527/jas.2006-799> PubMed PMID: ISI:000251814600001. PMID: 17785604
25. Ouni M, Gunes Y, Belot M-P, Castell A-L, Fradin D, Bougnères P. The *IGF1* P2 promoter is an epigenetic QTL for circulating IGF1 and human growth. *Clin Epigenetics*. 2015; 7(1):1–12. <https://doi.org/10.1186/s13148-015-0062-8> PMID: 25789079
26. Lonergan P, Gutierrez-Adan A, Pintado B, Fair T, Ward F, De La Fuente J, et al. Relationship between time of first cleavage and the expression of IGF-I growth factor, its receptor, and two housekeeping genes in bovine two-cell embryos and blastocysts produced in vitro. *Mol Reprod Dev*. 2000; 57(2):146–52. [https://doi.org/10.1002/1098-2795\(200010\)57:2<146::AID-MRD5>3.0.CO;2-2](https://doi.org/10.1002/1098-2795(200010)57:2<146::AID-MRD5>3.0.CO;2-2) PubMed PMID: WOS:000089086100005. PMID: 10984414
27. Lighten AD, Hardy K, Winston RML, Moore GE. Expression of mRNA for the insulin-like growth factors and their receptors in human preimplantation embryos. *Mol Reprod Dev*. 1997; 47(2):134–9. [https://doi.org/10.1002/\(SICI\)1098-2795\(199706\)47:2<134::AID-MRD2>3.0.CO;2-N](https://doi.org/10.1002/(SICI)1098-2795(199706)47:2<134::AID-MRD2>3.0.CO;2-N) PubMed PMID: WOS:A1997WW60700002. PMID: 9136113
28. Rotwein P, Pollock KM, Watson M, Milbrandt JD. Insulin-like growth factor gene expression during rat embryonic development. *Endocrinology*. 1987; 121(6):2141–4. <https://doi.org/10.1210/endo-121-6-2141> PMID: 3678142
29. Fu Q, Yu X, Callaway CW, Lane RH, McKnight RA. Epigenetics: intrauterine growth retardation (IGR) modifies the histone code along the rat hepatic IGF-1 gene. *FASEB J*. 2009; 23(8):2438–49. <https://doi.org/10.1096/fj.08-124768> PMID: 19364764
30. Jansen E, Steenbergh PH, Vanschaik FMA, Sussenbach JS. The human IGF-I gene contains two cell type-specifically regulated promoters. *Biochem Biophys Res Commun*. 1992; 187(3):1219–26. [https://doi.org/10.1016/0006-291x\(92\)90433-1](https://doi.org/10.1016/0006-291x(92)90433-1) PubMed PMID: WOS:A1992JQ81200003. PMID: 1417797
31. Dickson MC, Saunders JC, Gilmour RS. The ovine insulin-like growth factor-I gene: characterization, expression and identification of a putative promoter. *J Mol Endocrinol*. 1991; 6(1):17–31. <https://doi.org/10.1677/jme.0.0060017> PMID: 2015053
32. LeRoith D, Roberts CT. Insulin-like growth factor I (IGF-I): A molecular basis for endocrine versus local action? *Mol Cell Endocrinol*. 1991; 77(1):C57–C61. [https://doi.org/10.1016/0303-7207\(91\)90054-V](https://doi.org/10.1016/0303-7207(91)90054-V).
33. DeChiara TM, Robertson EJ, Efstratiadis A. Parental imprinting of the mouse insulin-like growth factor II gene. *Cell*. 1991; 64(4):849–59. PMID: 1997210
34. Giannoukakis N, Deal C, Paquette J, Goodyer CG, Polychronakos C. Parental genomic imprinting of the human IGF2 gene. *Nat Genet*. 1993; 4(1):98–101. <https://doi.org/10.1038/ng0593-98> PubMed PMID: WOS:A1993LA33700022. PMID: 8099843
35. McLaren RJ, Montgomery GW. Genomic imprinting of the insulin-like growth factor 2 gene in sheep. *Mamm Genome*. 1999; 10(6):588–91. PubMed PMID: ISI:000080383300012. PMID: 10341091

36. Dindot SV, Kent KC, Evers B, Loskutoff N, Womack J, Piedrahita JA. Conservation of genomic imprinting at the *XIST*, *IGF2*, and *GTL2* loci in the bovine. *Mamm Genome*. 2004; 15(12):966–74. <https://doi.org/10.1007/s00335-004-2407-z> PubMed PMID: ISI:000225371100004. PMID: 15599555
37. Vu TH, Hoffman AR. Promoter-specific imprinting of the human insulin-like growth factor-II gene. *Nature*. 1994; 371(6499):714–7. <https://doi.org/10.1038/371714a0> PMID: 7935819
38. Ekstrom TJ, Cui H, Li X, Ohlsson R. Promoter-specific *IGF2* imprinting status and its plasticity during human liver development. *Development*. 1995; 121(2):309–16. PMID: 7768174
39. Qi Y, Ma N, Yan F, Yu Z, Wu G, Qiao Y, et al. The expression of intronic miRNAs, miR-483 and miR-483*, and their host gene, *Igf2*, in murine osteoarthritis cartilage. *Intr J Biol Macromol*. 2013; 61:43–9. <https://doi.org/10.1016/j.ijbiomac.2013.06.006> PMID: 23791756
40. Ma N, Wang X, Qiao Y, Li F, Hui Y, Zou C, et al. Coexpression of an intronic microRNA and its host gene reveals a potential role for miR-483-5p as an *IGF2* partner. *Mol Cell Endocrinol*. 2011; 333(1):96–101. <https://doi.org/10.1016/j.mce.2010.11.027> PMID: 21146586
41. Qiao Y, Zhao Y, Liu Y, Ma N, Wang C, Zou J, et al. miR-483-3p regulates hyperglycaemia-induced cardiomyocyte apoptosis in transgenic mice. *Biochem Biophys Res Commun*. 2016; 477(4):541–7. <https://doi.org/10.1016/j.bbrc.2016.06.051> PMID: 27346130
42. Ohlsen SM, Lugenbeel KA, Wong EA. Characterization of the linked ovine insulin-like growth factor-II genes. *DNA Cell Biol*. 1994; 13(4):377–88. PubMed PMID: WOS:A1994NL87100006. <https://doi.org/10.1089/dna.1994.13.377> PMID: 8011164
43. Curchoe C, Zhang SQ, Bin YF, Zhang XQ, Yang L, Feng DY, et al. Promoter-specific expression of the imprinted *IGF2* gene in cattle (*Bos taurus*). *Biol Reprod*. 2005; 73(6):1275–81. <https://doi.org/10.1095/biolreprod.105.044727> PubMed PMID: WOS:000233580700024. PMID: 16120826
44. Amarger V, Nguyen M, Van Laere AS, Braunschweig M, Nezer C, Georges M, et al. Comparative sequence analysis of the *INS-IGF2-H19* gene cluster in pigs. *Mamm Genome*. 2002; 13(7):388–98. <https://doi.org/10.1007/s00335-001-3059-x> PubMed PMID: ISI:000177236700009. PMID: 12140686
45. Ohlsson R, Hedborg F, Holmgren L, Walsh C, Ekstrom TJ. Overlapping patterns of *IGF2* and *H19* expression during human development: biallelic *IGF2* expression correlates with a lack of *H19* expression. *Development*. 1994; 120(2):361–8. PubMed PMID: WOS:A1994MW03600012. PMID: 8149914
46. Depagterholthuisen P, Jansen M, Vanschaik FMA, Vanderkammen R, Oosterwijk C, Vandenbrande JL, et al. The human insulin-like growth factor-II gene contains 2 development-specific promoters. *FEBS Lett*. 1987; 214(2):259–64. PubMed PMID: WOS:A1987H130300007. PMID: 3569524
47. van Dijk MA, van Schaik FMA, Bootsma HJ, Holthuisen P, Sussenbach JS. Initial characterization of the four promoters of the human insulin-like growth factor II gene. *Mol Cell Endocrinol*. 1991; 81(1):81–94. [https://doi.org/10.1016/0303-7207\(91\)90207-9](https://doi.org/10.1016/0303-7207(91)90207-9).
48. Holthuisen PE, Cleutjens CBJM, Veenstra GJC, van der Lee FM, Koonen-Reemst AMCB, Sussenbach JS. Differential expression of the human, mouse and rat IGF-II genes. *Regul Pept*. 1993; 48(1–2):77–89. PMID: 8265819
49. Moore T, Constancia M, Zubair M, Bailleul B, Feil R, Sasaki H, et al. Multiple imprinted sense and anti-sense transcripts, differential methylation and tandem repeats in a putative imprinting control region upstream of mouse *Igf2*. *Proc Natl Acad Sci U S A*. 1997; 94(23):12509–14. PubMed PMID: WOS: A1997YF39300049. PMID: 9356480
50. Monk D, Sanches R, Arnaud P, Apostolidou S, Hills FA, Abu-Amro S, et al. Imprinting of *IGF2* P0 transcript and novel alternatively spliced *INS-IGF2* isoforms show differences between mouse and human. *Hum Mol Genet*. 2006; 15(8):1259–69. <https://doi.org/10.1093/hmg/ddl041> PubMed PMID: WOS:000236613300002. PMID: 16531418
51. Tran VG, Court F, Duputié A, Antoine E, Aptel N, Milligan L, et al. *H19* antisense RNA can up-regulate *Igf2* transcription by activation of a novel promoter in mouse myoblasts. *PLoS One*. 2012; 7(5): e37923. <https://doi.org/10.1371/journal.pone.0037923> PMID: 22662250
52. Engel N, West AG, Felsenfeld G, Bartolomei MS. Antagonism between DNA hypermethylation and enhancer-blocking activity at the *H19* DMD is uncovered by CpG mutations. *Nat Genet*. 2004; 36(8):883–8. <https://doi.org/10.1038/ng1399> PMID: 15273688
53. Ainscough JFX, Dandolo L, Azim Surani M. Appropriate expression of the mouse *H19* gene utilises three or more distinct enhancer regions spread over more than 130 kb. *Mech Dev*. 2000; 91(1–2):365–8. [https://doi.org/10.1016/S0925-4773\(99\)00289-0](https://doi.org/10.1016/S0925-4773(99)00289-0) PMID: 10704866
54. Bartolomei MS, Zemel S, Tilghman SM. Parental imprinting of the mouse *H19* gene. *Nature*. 1991; 351(6322):153–5. <https://doi.org/10.1038/351153a0> PMID: 1709450
55. Zhang SQ, Kubota C, Yang L, Zhang YQ, Page R, O'Neill M, et al. Genomic imprinting of *H19* in naturally reproduced and cloned cattle. *Biol Reprod*. 2004; 71(5):1540–4. <https://doi.org/10.1095/biolreprod.104.031807> PubMed PMID: ISI:000224713000018. PMID: 15240429

56. Li C, Bin YF, Curchoe C, Yang L, Feng DY, Jiang QY, et al. Genetic imprinting of *H19* and *IGF2* in domestic pigs (*Sus scrofa*). *Anim Biotechnol*. 2008; 19(1):22–7. <https://doi.org/10.1080/10495390701758563> PubMed PMID: WOS:000258687500003. PMID: 18228173
57. Keniry A, Oxley D, Monnier P, Kyba M, Dandolo L, Smits G, et al. The *H19* lincRNA is a developmental reservoir of miR-675 that suppresses growth and *Igf1r*. *Nat Cell Biol*. 2012; 14(7):659–65. <http://www.nature.com/ncb/journal/v14/n7/abs/ncb2521.html#supplementary-information>. PMID: 22684254
58. Xiang R, Lee AMC, Eindorf T, Javadmanesh A, Ghanipoor-Samami M, Gugger M, et al. Widespread differential maternal and paternal genome effects on fetal bone phenotype at mid-gestation. *J Bone Miner Res*. 2014; 29(11):2392–404. <https://doi.org/10.1002/jbmr.2263> PMID: 24753181
59. Xiang R, Ghanipoor-Samami M, Johns WH, Eindorf T, Rutley DL, Kruk ZA, et al. Maternal and paternal genomes differentially affect myofibre characteristics and muscle weights of bovine fetuses at mid-gestation. *PLoS One*. 2013; 8(1):e53402. <https://doi.org/10.1371/journal.pone.0053402> PMID: 23341941
60. Moller DE, Yokota A, Caro JF, Flier JS. Tissue-specific expression of two alternatively spliced insulin receptor mRNAs in man. *Mol Endocrinol*. 1989; 3(8):1263–9. PubMed PMID: WOS: A1989AL93900012. <https://doi.org/10.1210/mend-3-8-1263> PMID: 2779582
61. Pollak M. The insulin and insulin-like growth factor receptor family in neoplasia: an update. *Nat Rev Cancer*. 2012; 12(3):159–69. <https://doi.org/10.1038/nrc3215> PubMed PMID: WOS:000300833600009. PMID: 22337149
62. Mosthaf L, Grako K, Dull TJ, Coussens L, Ullrich A, McClain DA. Functionally distinct insulin receptors generated by tissue-specific alternative splicing. *EMBO J*. 1990; 9(8):2409–13. PubMed PMID: WOS: A1990DP59500008. PMID: 2369896
63. Pandini G, Frasca F, Mineo F, Sciacca P, Vigneri R, Belfiore A. Insulin/insulin-like growth factor I hybrid receptors have different biological characteristics depending on the insulin receptor isoform involved. *J Biol Chem*. 2002; 277:39684–95. <https://doi.org/10.1074/jbc.M202766200> PMID: 12138094
64. Belfiore A, Frasca F, Pandini G, Sciacca L, Vigneri R. Insulin receptor isoforms and insulin receptor/insulin-like growth factor receptor hybrids in physiology and disease. *Endocr Rev*. 2009; 30(6):586–623. <https://doi.org/10.1210/er.2008-0047> PMID: 19752219.
65. Frasca F, Pandini G, Scalia P, Sciacca L, Mineo R, Costantino A, et al. Insulin receptor isoform A, a newly recognized, high-affinity insulin-like growth factor II receptor in fetal and cancer cells. *Mol Cell Biol*. 1999; 19(5):3278–88. PMID: 10207053
66. Leroith D, Werner H, Beitnerjohnson D, Roberts CT. Molecular and cellular aspects of the insulin-like growth-factor-I receptor. *Endocr Rev*. 1995; 16(2):143–63. PubMed PMID: WOS:A1995QT90200002. <https://doi.org/10.1210/edrv-16-2-143> PMID: 7540132
67. Belfiore A, Malaguarnera R, Vella V, Lawrence MC, Sciacca L, Frasca F, et al. Insulin receptor isoforms in physiology and disease: An updated view. *Endocr Rev*. 2017; 38(5):379–431. <https://doi.org/10.1210/er.2017-00073> PMID: 28973479
68. Hwa V, Fang P, Derr MA, Fiegerlova E, Rosenfeld RG. IGF-I in human growth: lessons from defects in the GH-IGF-I axis. In: Gillman MW, Gluckman PD, Rosenfeld RG, editors. *Recent Advances in Growth Research: Nutritional, Molecular and Endocrine Perspectives*. Nestle Nutrition Institute Workshop Series. 712013. p. 43–55.
69. Jospe N, Kaplowitz PB, Furlanetto RW. Homozygous nonsense mutation in the insulin receptor gene of a patient with severe congenital insulin resistance: Leprechaunism and the role of the insulin-like growth factor receptor. *Clin Endocrinol (Oxf)*. 1996; 45(2):229–35. PubMed PMID: WOS: A1996VD87300016.
70. Louvi A, Accili D, Efstratiadis A. Growth-promoting interaction of IGF-II with the insulin receptor during mouse embryonic development. *Dev Biol*. 1997; 189(1):33–48. <https://doi.org/10.1006/dbio.1997.8666>. PMID: 9281335
71. Ghosh P, Dahms NM, Kornfeld S. Mannose 6-phosphate receptors: new twists in the tale. *Nat Rev Mol Cell Biol*. 2003; 4(3):202–13. <https://doi.org/10.1038/nrm1050> PMID: 12612639
72. McKinnon T, Chakraborty C, Gleeson LM, Chidiac P, Lala PK. Stimulation of human extravillous trophoblast migration by IGF-II is mediated by IGF Type 2 receptor involving inhibitory G protein(s) and phosphorylation of MAPK. *J Clin Endocrinol Metab*. 2001; 86(8):3665–74. <https://doi.org/10.1210/jcem.86.8.7711> PMID: 11502794
73. Barlow DP, Stoger R, Herrmann BG, Saito K, Schweifer N. The mouse insulin-like growth factor type-2 receptor is imprinted and closely linked to the *Tme* locus. *Nature*. 1991; 349(6304):84–7. <https://doi.org/10.1038/349084a0> PMID: 1845916
74. Killian JK, Nolan CM, Wylie AA, Li T, Vu TH, Hoffman AR, et al. Divergent evolution in *M6P/IGF2R* imprinting from the Jurassic to the Quaternary. *Hum Mol Genet*. 2001; 10(17):1721–8. PubMed PMID: ISI:000171125600001. PMID: 11532981

75. Young LE, Schnieke AE, McCreath KJ, Wieckowski S, Konfortova G, Fernandes K, et al. Conservation of *IGF2-H19* and *IGF2R* imprinting in sheep: effects of somatic cell nuclear transfer. *Mech Dev.* 2003; 120(12):1433–42. PMID: [14654216](#)
76. Xu YQ, Goodyer CG, Deal C, Polychronakos C. Functional polymorphism in the parental imprinting of the human *IGF2R* gene. *Biochem Biophys Res Commun.* 1993; 197(2):747–54. PubMed PMID: WOS:A1993MM43600057. PMID: [8267611](#)
77. Bebbere D, Bauersachs S, Fürst RW, Reichenbach H-D, Reichenbach M, Medugorac I, et al. Tissue-specific and minor inter-individual variation in imprinting of *IGF2R* is a common feature of *Bos taurus* concepti and not correlated with fetal weight. *PLoS One.* 2013; 8(4):e59564. <https://doi.org/10.1371/journal.pone.0059564> PMID: [23593146](#)
78. Wang ZQ, Fung MR, Barlow DP, Wagner EF. Regulation of embryonic growth and lysosomal targeting by the imprinted *Igf2/Mpr* gene. *Nature.* 1994; 372(6505):464–7. PubMed PMID: WOS: A1994PV01200057. <https://doi.org/10.1038/372464a0> PMID: [7984240](#)
79. Berkowicz EW, Magee DA, Berry DP, Sikora KM, Howard DJ, Mullen MP, et al. Single nucleotide polymorphisms in the imprinted bovine *insulin-like growth factor 2 receptor* gene (*IGF2R*) are associated with body size traits in Irish Holstein-Friesian cattle. *Anim Genet.* 2012; 43(1):81–7. <https://doi.org/10.1111/j.1365-2052.2011.02211.x> PMID: [22221028](#)
80. Farmer WT, Farin PW, Piedrahita JA, Bischoff SR, Farin CE. Expression of antisense of insulin-like growth factor-2 receptor RNA non-coding (*AIRM*) during early gestation in cattle. *Anim Reprod Sci.* 2013; 138(1–2):64–73. <https://doi.org/10.1016/j.anireprosci.2013.01.009>. PMID: [23473694](#)
81. Latos PA, Pauler FM, Koerner MV, Şenergin HB, Hudson QJ, Stocsits RR, et al. *Airm* transcriptional overlap, but not its lncRNA products, induces imprinted *Igf2r* silencing. *Science.* 2012; 338(6113):1469–72. <https://doi.org/10.1126/science.1228110> PMID: [23239737](#)
82. Yotova IY, Vlatkovic IM, Pauler FM, Warczok KE, Ambros PF, Oshimura M, et al. Identification of the human homolog of the imprinted mouse *Air* non-coding RNA. *Genomics.* 2008; 92(6):464–73. <https://doi.org/10.1016/j.ygeno.2008.08.004> PMID: [18789384](#)
83. Hwa V, Oh Y, Rosenfeld RG. The insulin-like growth factor-binding protein (IGFBP) superfamily. *Endocr Rev.* 1999; 20(6):761–87. <https://doi.org/10.1210/edrv.20.6.0382> PMID: [10605625](#).
84. Firth SM, Baxter RC. Cellular actions of the insulin-like growth factor binding proteins. *Endocr Rev.* 2002; 23(6):824–54. <https://doi.org/10.1210/er.2001-0033> PMID: [12466191](#).
85. Wood TL, Rogler LE, Czick ME, Schuller AGP, Pintar JE. Selective alterations in organ sizes in mice with a targeted disruption of the insulin-like growth factor binding protein-2 gene. *Mol Endocrinol.* 2000; 14(9):1472–82. <https://doi.org/10.1210/mend.14.9.0517> PubMed PMID: WOS:000089093600014. PMID: [10976924](#)
86. Murali SG, Brinkman AS, Solverson P, Pun W, Pintar JE, Ney DM. Exogenous GLP-2 and IGF-I induce a differential intestinal response in IGF binding protein-3 and-5 double knockout mice. *Am J Physiol Gastrointest Liver Physiol.* 2012; 302(8):G794–G804. <https://doi.org/10.1152/ajpgi.00372.2011> PubMed PMID: WOS:000302918300005. PMID: [22281475](#)
87. Silha JV, Murphy LJ. Minireview: Insights from insulin-like growth factor binding protein transgenic mice. *Endocrinology.* 2002; 143(10):3711–4. <https://doi.org/10.1210/en.2002-220116> PubMed PMID: WOS:000178212800001. PMID: [12239079](#)
88. Kostecka Z, Blahovec J. Animal insulin-like growth factor binding proteins and their biological functions. *Vet Med (Praha).* 2002; 47(2–3):75–84. PubMed PMID: WOS:000175865800007.
89. Ivkovic S, Yoon BS, Popoff SN, Safadi FF, Libuda DE, Stephenson RC, et al. Connective tissue growth factor coordinates chondrogenesis and angiogenesis during skeletal development. *Development.* 2003; 130(12):2779–91. <https://doi.org/10.1242/dev.00505> PubMed PMID: WOS:000183759600020. PMID: [12736220](#)
90. Schofield PN, Tate VE. Regulation of human IGF-II transcription in fetal and adult tissues. *Development.* 1987; 101(4):793–803. PMID: [3503697](#)
91. O'Mahoney JV, Brandon MR, Adams TE. Developmental and tissue-specific regulation of ovine insulin-like growth factor II (IGF-II) mRNA expression. *Mol Cell Endocrinol.* 1991; 78(1–2):87–96. PMID: [1936528](#)
92. Boulle N, Schneid H, Listrat A, Holthuisen P, Binoux M, Groyer A. Developmental regulation of bovine insulin-like growth factor-II (IGF-II) gene-expression—Homology between bovine transcripts and human IGF-II exons. *J Mol Endocrinol.* 1993; 11(2):117–28. PubMed PMID: WOS: A1993MG25500001. PMID: [8297468](#)
93. Alfieri CM, Evans-Anderson HJ, Yutzey KE. Developmental regulation of the mouse IGF-I exon 1 promoter region by calcineurin activation of NFAT in skeletal muscle. *Am J Physiol Cell Physiol.* 2007; 292(5):C1887–C94. <https://doi.org/10.1152/ajpcell.00506.2006> PMID: [17229811](#)

94. Li ZC, Wu ZF, Ren GC, Zhao YX, Liu DW. Expression patterns of insulin-like growth factor system members and their correlations with growth and carcass traits in Landrace and Lantang pigs during postnatal development. *Mol Biol Rep.* 2013; 40(5):3569–76. <https://doi.org/10.1007/s11033-012-2430-1> PubMed PMID: WOS:000317075300012. PMID: 23269622
95. Werner H, Woloschak M, Adamo M, Shen-Orr Z, Roberts CT, LeRoith D. Developmental regulation of the rat insulin-like growth factor I receptor gene. *Proc Natl Acad Sci U S A.* 1989; 86(19):7451–5. PMID: 2477843
96. Nissley P, Kiess W, Sklar M. Developmental expression of the IGF-II/mannose 6-phosphate receptor. *Mol Reprod Dev.* 1993; 35(4):408–13. <https://doi.org/10.1002/mrd.1080350415> PMID: 8398120
97. Fowden AL. The insulin-like growth factors and feto-placental growth. *Placenta.* 2003; 24(8):803–12. [https://doi.org/10.1016/S0143-4004\(03\)00080-8](https://doi.org/10.1016/S0143-4004(03)00080-8).
98. Delhanty PJ, Han VK. The expression of insulin-like growth factor (IGF)-binding protein-2 and IGF-II genes in the tissues of the developing ovine fetus. *Endocrinology.* 1993; 132(1):41–52. <https://doi.org/10.1210/endo.132.1.7678219> PMID: 7678219
99. Lee CY, Chung CS, Simmen FA. Ontogeny of the porcine insulin-like growth factor system. *Mol Cell Endocrinol.* 1993; 93(1):71–80. [https://doi.org/10.1016/0303-7207\(93\)90141-6](https://doi.org/10.1016/0303-7207(93)90141-6). PMID: 7686518
100. Gerrard DE, Okamura CS, Grant AL. Expression and location of IGF binding proteins-2, -4, and -5 in developing fetal tissues. *J Anim Sci.* 1999; 77(6):1431–41. PMID: 10375221
101. Anand-Ivell R, Hiendleder S, Viñoles C, Martin GB, Fitzsimmons C, Eurich A, et al. INSL3 in the ruminant: A powerful indicator of gender- and genetic-specific feto-maternal dialogue. *PLoS One.* 2011; 6(5):e19821. <https://doi.org/10.1371/journal.pone.0019821> PMID: 21603619
102. Altschul SF, Gish W, Miller W, Myers EW, Lipman DJ. Basic local alignment search tool. *J Mol Biol.* 1990; 215(3):403–10. [https://doi.org/10.1016/S0022-2836\(05\)80360-2](https://doi.org/10.1016/S0022-2836(05)80360-2) PubMed PMID: WOS: A1990ED16700008. PMID: 2231712
103. Bustin SA, Benes V, Garson JA, Hellemans J, Huggett J, Kubista M, et al. The MIQE guidelines: minimum information for publication of quantitative real-time PCR experiments. *Clin Chem.* 2009; 55(4):611–22. <https://doi.org/10.1373/clinchem.2008.112797> PMID: 19246619
104. Johnson JW. A heuristic method for estimating the relative weight of predictor variables in multiple regression. *Multivariate Behav Res.* 2000; 35(1):1–19. https://doi.org/10.1207/S15327906MBR3501_1 PMID: 26777229
105. Johnson JW. Factors affecting relative weights: the influence of sampling and measurement Error. *Organ Res Methods.* 2004; 7(3):283–99. <https://doi.org/10.1177/1094428104266018>
106. Andersen CL, Jensen JL, Ørntoft TF. Normalization of real-time quantitative reverse transcription-PCR data: a model-based variance estimation approach to identify genes suited for normalization, applied to bladder and colon cancer data sets. *Cancer Res.* 2004; 64(15):5245–50. <https://doi.org/10.1158/0008-5472.CAN-04-0496> PMID: 15289330
107. Vandesompele J, De Preter K, Pattyn F, Poppe B, Van Roy N, De Paepe A, et al. Accurate normalization of real-time quantitative RT-PCR data by geometric averaging of multiple internal control genes. *Genome Biology.* 2002; 3(7):research0034.1—research.11. PubMed PMID: <https://doi.org/10.1186/gb-2002-3-7-research0034>
108. Lorenzo-Seva U, Ferrando P, Chico E. Two SPSS programs for interpreting multiple regression results. *Behav Res Methods.* 2010; 42(1):29–35. <https://doi.org/10.3758/BRM.42.1.29> PMID: 20160283
109. Ohlsson C, Mohan S, Sjögren K, Tivesten Å, Isgaard J, Isaksson O, et al. The role of liver-derived insulin-like growth factor-I. *Endocr Rev.* 2009; 30(5):494–535. <https://doi.org/10.1210/er.2009-0010> PMID: 19589948.
110. Pell JM, Saunders JC, Gilmour RS. Differential regulation of transcription initiation from insulin-like growth factor-I (IGF-I) leader exons and of tissue IGF-I expression in response to changed growth hormone and nutritional status in sheep. *Endocrinology.* 1993; 132(4):1797–807. <https://doi.org/10.1210/endo.132.4.8462477> PMID: 8462477
111. Ohtsuki T, Otsuki M, Murakami Y, Maekawa T, Yamamoto T, Akasaka K, et al. Organ-specific and age-dependent expression of insulin-like growth factor-I (IGF-I) mRNA variants: IGF-IA and IB mRNAs in the mouse. *Zoolog Sci.* 2005; 22(9):1011–21. <https://doi.org/10.2108/zsj.22.1011> PMID: 16219982
112. Bornfeldt KE, Arnqvist HJ, Enberg B, Mathews LS, Norstedt G. Regulation of insulin-like growth factor-I and growth hormone receptor gene expression by diabetes and nutritional state in rat tissues. *J Endocrinol.* 1989; 122(3):651–6. <https://doi.org/10.1677/joe.0.1220651> PMID: 2809476
113. Lund PK, Moatsstaats BM, Hynes MA, Simmons JG, Jansen M, Dercole AJ, et al. Somatomedin-C/insulin-like growth factor-I and insulin-like growth factor-II mRNAs in rat fetal and adult tissues. *J Biol Chem.* 1986; 261(31):4539–44. PubMed PMID: WOS:A1986E668100028.

114. Murphy LJ, Bell GI, Duckworth ML, Friesen HG. Identification, characterization, and regulation of a rat complementary deoxyribonucleic acid which encodes insulin-like growth factor-I. *Endocrinology*. 1987; 121(2):684–91. PubMed PMID: WOS:A1987J303900033. <https://doi.org/10.1210/endo-121-2-684> PMID: 3595538
115. Liu J-P, Baker J, Perkins AS, Robertson EJ, Efstratiadis A. Mice carrying null mutations of the genes encoding insulin-like growth factor I (*Igf-1*) and type 1 IGF receptor (*Igf1r*). *Cell*. 1993; 75(1):59–72. [https://doi.org/10.1016/S0092-8674\(05\)80084-4](https://doi.org/10.1016/S0092-8674(05)80084-4). PMID: 8402901
116. Hiendleder S, Wirtz M, Mund C, Klempt M, Reichenbach H-D, Stojkovic M, et al. Tissue-specific effects of in vitro fertilization procedures on genomic cytosine methylation levels in overgrown and normal sized bovine fetuses. *Biol Reprod*. 2006; 75(1):17–23. <https://doi.org/10.1095/biolreprod.105.043919> PMID: 16554415
117. Kind KL, Owens JA, Robinson JS, Quinn KJ, Grant PA, Walton PE, et al. Effect of restriction of placental growth on expression of IGFs in fetal sheep: relationship to fetal growth, circulating IGFs and binding proteins. *J Endocrinol*. 1995; 146(1):23–34. <https://doi.org/10.1677/joe.0.1460023> PMID: 7561617
118. Shen W, Wisniewski P, Ahmed L, Boyle DW, Denne SC, Liechty EA. Protein anabolic effects of insulin and IGF-I in the ovine fetus. *Am J Physiol Endocrinol Metab*. 2003; 284(4):E748–E56. <https://doi.org/10.1152/ajpendo.00399.2002> PMID: 12488244
119. Wang Y, Price SE, Jiang H. Cloning and characterization of the bovine class 1 and class 2 insulin-like growth factor-I mRNAs. *Domest Anim Endocrinol*. 2003; 25(4):315–28. <https://doi.org/10.1016/j.domaniend.2003.06.001> PMID: 14652133
120. Zhang J, Zhang G, Yang R, Niu S, Bai W, Liu D, et al. Cloning and characterization of four new splice variants of insulin-like growth factor-I gene in Chinese red steppes. *Journal of Animal and Veterinary Advances*. 2011; 10(18):2459–64. <https://doi.org/10.3923/javaa.2011.2459.2464>
121. O'Sullivan DC, Szeszak TAM, Pell JM. Regulation of hepatic insulin-like growth factor I leader exon usage in lambs: effect of immunization against growth hormone-releasing factor and subsequent growth hormone treatment. *J Anim Sci*. 2002; 80(4):1074–82. PubMed PMID: WOS:000174808700027. PMID: 12002314
122. Xiao S, Li S, Zhang J, Zhang S, Dai L, Bao Y, et al. Cloning and characterization of class 1 and class 2 insulin-like growth factor-I mRNA in Songliao black pig. *Mol Biol Rep*. 2009; 36(2):415–21. <https://doi.org/10.1007/s11033-007-9195-y> PMID: 18157703
123. Weller PA, Dickson MC, Huskisson NS, Dauncey MJ, Buttery PJ, Gilmour RS. The porcine insulin-like growth factor-I gene: characterization and expression of alternate transcription sites. *J Mol Endocrinol*. 1993; 11(2):201–11. <https://doi.org/10.1677/jme.0.0110201> PMID: 8297476
124. Ohtsuki T, Otsuki M, Murakami Y, Hirata K, Takeuchi S, Takahashi S. Alternative leader-exon usage in mouse IGF-I mRNA variants: Class 1 and class 2 IGF-I mRNAs. *Zoolog Sci*. 2007; 24(3):241–7. <https://doi.org/10.2108/zsj.24.241> PubMed PMID: WOS:000246994800005. PMID: 17551244
125. Shemer J, Adamo ML, C T Roberts J, LeRoith D. Tissue-specific transcription start site usage in the leader exons of the rat insulin-like growth factor-I gene: evidence for differential regulation in the developing kidney. *Endocrinology*. 1992; 131(6):2793–9. <https://doi.org/10.1210/endo.131.6.1446616> PMID: 1446616.
126. Randhawa R, Cohen P. The role of the insulin-like growth factor system in prenatal growth. *Mol Genet Metab*. 2005; 86:84–90. <https://doi.org/10.1016/j.ymgme.2005.07.028> PMID: 16165387
127. Constancia M, Hemberger M, Hughes J, Dean W, Ferguson-Smith A, Fundele R, et al. Placental-specific IGF-II is a major modulator of placental and fetal growth. *Nature*. 2002; 417(6892):945–8. PubMed PMID: WOS:000176441200038. <https://doi.org/10.1038/nature00819> PMID: 12087403
128. Fowden AL, Sibley C, Reik W, Constancia M. Imprinted genes, placental development and fetal growth. *Horm Res Paediatr*. 2006; 65(suppl 3)(Suppl. 3):50–8.
129. Huang Y-Z, Zhan Z-Y, Sun Y-J, Cao X-K, Li M-X, Wang J, et al. Intragenic DNA methylation status down-regulates bovine *IGF2* gene expression in different developmental stages. *Gene*. 2014; 534(2):356–61. <https://doi.org/10.1016/j.gene.2013.09.111>. PMID: 24140490
130. Soares MB, Turken A, Ishii D, Mills L, Episkopou V, Cotter S, et al. Rat insulin-like growth factor II gene: A single gene with two promoters expressing a multitranscript family. *J Mol Biol*. 1986; 192(4):737–52. PMID: 2438416
131. Gray A, Tam AW, Dull TJ, Hayflick J, Pintar J, Cavenee WK, et al. Tissue-specific and developmentally regulated transcription of the insulin-like growth factor-II gene. *DNA-A Journal of Molecular and Cellular Biology*. 1987; 6(4):283–95. <https://doi.org/10.1089/dna.1987.6.283> PubMed PMID: WOS: A1987J730900001. PMID: 3652904
132. Sullivan TM, Micke GC, Perkins N, Martin GB, Wallace CR, Gattford KL, et al. Dietary protein during gestation affects maternal insulin-like growth factor, insulin-like growth factor binding protein, leptin

- concentrations, and fetal growth in heifers. *J Anim Sci.* 2009; 87(10):3304–16. <https://doi.org/10.2527/jas.2008-1753> PMID: 19617516
133. Davies SM. Developmental regulation of genomic imprinting of the IGF2 gene in human liver. *Cancer Res.* 1994; 54(10):2560–2. PMID: 8168079
 134. Holthuizen P, van der Lee FM, Ikejiri K, Yamamoto M, Sussenbach JS. Identification and initial characterization of a fourth leader exon and promoter of the human IGF-II gene. *Biochim Biophys Acta.* 1990; 1087(3):341–3. PMID: 2248982
 135. Li X, Cui H, Sandstedt B, Nordlinder H, Larsson E, Ekstrom TJ. Expression levels of the insulin-like growth factor-II gene (IGF2) in the human liver: Developmental relationships of the four promoters. *J Endocrinol.* 1996; 149(1):117–24. PubMed PMID: WOS:A1996UD87000014. PMID: 8676043
 136. Sussenbach JS, Steenbergh PH, Holthuizen P. Structure and expression of the human insulin-like growth factor genes. *Growth Regul.* 1992; 2(1):1–9. PMID: 1486331.
 137. Frasca F, Pandini G, Sciacca L, Pezzino V, Squatrito S, Belfiore A, et al. The role of insulin receptors and IGF-I receptors in cancer and other diseases. *Archives of Physiology and Biochemistry.* 2008; 114(1):23–37. <https://doi.org/10.1080/13813450801969715> PMID: 18465356
 138. Accili D, Drago J, Lee EJ, Johnson MD, Cool MH, Salvatore P, et al. Early neonatal death in mice homozygous for a null allele of the insulin receptor gene. *Nat Genet.* 1996; 12(1):106–9. <https://doi.org/10.1038/ng0196-106> PMID: 8528241
 139. Ludwig T, Eggenschwiler J, Fisher P, Dercole AJ, Davenport ML, Efstratiadis A. Mouse mutants lacking the type 2 IGF receptor (IGF2R) are rescued from perinatal lethality in *Igf2* and *Igf1r* null backgrounds. *Dev Biol.* 1996; 177(2):517–35. PubMed PMID: WOS:A1996VA82900012. <https://doi.org/10.1006/dbio.1996.0182> PMID: 8806828
 140. Pellegrini M, Pilia G, Pantano S, Lucchini F, Uda M, Fumi M, et al. *Gpc3* expression correlates with the phenotype of the Simpson-Golabi-Behmel syndrome. *Dev Dyn.* 1998; 213(4):431–9. [https://doi.org/10.1002/\(SICI\)1097-0177\(199812\)213:4<431::AID-AJA8>3.0.CO;2-7](https://doi.org/10.1002/(SICI)1097-0177(199812)213:4<431::AID-AJA8>3.0.CO;2-7) PubMed PMID: WOS:000077534500008. PMID: 9853964
 141. El-Shewy HM, Lee M-H, Obeid LM, Jaffa AA, Luttrell LM. The insulin-like growth factor type 1 and insulin-like growth factor type 2/mannose-6-phosphate receptors independently regulate ERK1/2 activity in HEK293 cells. *J Biol Chem.* 2007; 282(36):26150–7. <https://doi.org/10.1074/jbc.M703276200> PMID: 17620336
 142. Chu C-H, Tzang B-S, Chen L-M, Kuo C-H, Cheng Y-C, Chen L-Y, et al. IGF-II/mannose-6-phosphate receptor signaling induced cell hypertrophy and atrial natriuretic peptide/BNP expression via Gαq interaction and protein kinase C-α/CaMKII activation in H9c2 cardiomyoblast cells. *J Endocrinol.* 2008; 197(2):381–90. <https://doi.org/10.1677/JOE-07-0619> PMID: 18434368
 143. Schuller AGP, Vanneck JW, Lindenberghkortelev DJ, Groffen C, Dejong I, Zwarthoff EC, et al. Gene expression of the IGF binding proteins during post-implantation embryogenesis of the mouse; comparison with the expression of IGF-I and -II and their receptors in rodent and human. In: LeRoith D, Razada MK, editors. *Current Directions in Insulin-Like Growth Factor Research. Advances in Experimental Medicine and Biology.* 3431993. p. 267–77.
 144. Han VKM, Matsell DG, Delhanty PJD, Hill DJ, Shimasaki S, Nygard K. IGF-binding protein mRNAs in the human fetus: tissue and cellular distribution of developmental expression. *Horm Res Paediatr.* 1996; 45(3–5):160–6.
 145. Ooi GT, Orlowski CC, Brown AL, Becker RE, Unterman TG, Rechler MM. Different tissue distribution and hormonal regulation of messenger RNAs encoding rat insulin-like growth factor-binding proteins-1 and -2. *Mol Endocrinol.* 1990; 4(2):321–8. PubMed PMID: BIOSIS:PREV199089103275. <https://doi.org/10.1210/mend-4-2-321> PMID: 1691819
 146. Murphy LJ, Seneviratne C, Ballejo G, Croze F, Kennedy TG. Identification and characterization of a rat decidua insulin-like growth factor-binding protein complementary DNA. *Mol Endocrinol.* 1990; 4(2):329–36. PubMed PMID: WOS:A1990CR02700019. <https://doi.org/10.1210/mend-4-2-329> PMID: 1691820
 147. Lewitt MS, Denyerf GS, Cooney J G, Baxter RC. Insulin-like growth factor-binding protein-1 modulates blood glucose levels. *Endocrinology.* 1991; 129(4):2254–6. <https://doi.org/10.1210/endo-129-4-2254> PMID: 1717244
 148. Brismar K, Fernqvist-Forbes E, Wahren J, Hall K. Effect of insulin on the hepatic production of insulin-like growth factor-binding protein-1 (IGFBP-1), IGFBP-3, and IGF-I in insulin-dependent diabetes. *J Clin Endocrinol Metab.* 1994; 79(3):872–8. <https://doi.org/10.1210/jcem.79.3.7521354> PMID: 7521354
 149. Lee PDK, Conover CA, Powell DR. Regulation and function of insulin-like growth factor-binding protein-1. *Proc Soc Exp Biol Med.* 1993; 204(1):4–29. <https://doi.org/10.3181/00379727-204-43630> PMID: 7690486

150. Hall K, Brismar K, Grissom F, Lindgren B, Pova G. IGFBP-1. Production and control mechanisms. *Acta Endocrinol (Copenh)*. 1991; 124:48–54. PubMed PMID: WOS:A1991FV94700009.
151. Donovan SM, Oh Y, Pham H, Rosenfeld RG. Ontogeny of serum insulin-like growth factor binding proteins in the rat. *Endocrinology*. 1989; 125(5):2621–7. <https://doi.org/10.1210/endo-125-5-2621> PMID: 2477234.
152. Lassarre C, Hardouin S, Daffos F, Forestier F, Frankenne F, Binoux M. Serum insulin-like growth factors and insulin-like growth factor binding proteins in the human fetus. relationships with growth in normal subjects and in subjects with intrauterine growth retardation. *Pediatr Res*. 1991; 29(3):219–25. <https://doi.org/10.1203/00006450-199103000-00001> PMID: 1709729
153. Lee CY, Bazer FW, Etherton TD, Simmen FA. Ontogeny of insulin-like growth factors (IGF-I and IGF-II) and IGF-binding proteins in porcine serum during fetal and postnatal development. *Endocrinology*. 1991; 128(5):2336–44. <https://doi.org/10.1210/endo-128-5-2336> PMID: 1708333.
154. Liu F, Powell DR, Styne DM, Hintz RL. Insulin-like growth factors (IGFs) and IGF-binding proteins in the developing rhesus monkey. *J Clin Endocrinol Metab*. 1991; 72(4):905–11. <https://doi.org/10.1210/jcem-72-4-905> PMID: 1706351.
155. Carr JM, Owens JA, Grant PA, Walton PE, Owens PC, Wallace JC. Circulating insulin-like growth factors (IGFs), IGF-binding proteins (IGFBPs) and tissue mRNA levels of IGFBP-2 and IGFBP-4 in the ovine fetus. *J Endocrinol*. 1995; 145(3):545–57. <https://doi.org/10.1677/joe.0.1450545> PubMed PMID: WOS:A1995RB15700018. PMID: 7543554
156. Han VKM, Carter AM. Spatial and temporal patterns of expression of messenger RNA for insulin-like growth factors and their binding proteins in the placenta of man and laboratory animals. *Placenta*. 2000; 21(4):289–305. <https://doi.org/10.1053/plac.1999.0498>. PMID: 10833363
157. Coulter CL, Han VKM. The pattern of expression of insulin-like growth factor (IGF), IGF-I receptor and IGF binding protein (IGFBP) mRNAs in the rhesus monkey placenta suggests a paracrine mode of IGF-IGFBP interaction in placental development. *Placenta*. 1996; 17(7):451–60. PubMed PMID: WOS:A1996VL49500009. PMID: 8899874
158. Miyakoshi N, Qin X, Kasukawa Y, Richman C, Srivastava AK, Baylink DJ, et al. Systemic administration of insulin-like growth factor (IGF)-binding protein-4 (IGFBP-4) increases bone formation parameters in mice by increasing IGF bioavailability via an IGFBP-4 protease-dependent mechanism. *Endocrinology*. 2001; 142(6):2641–8. <https://doi.org/10.1210/endo.142.6.8192> PMID: 11356715.
159. Bach LA, Salemi R, Leeding KS. Roles of insulin-like growth factor (IGF) receptors and IGF-binding proteins in IGF-II-induced proliferation and differentiation of L6A1 rat myoblasts. *Endocrinology*. 1995; 136(11):5061–9. <https://doi.org/10.1210/endo.136.11.7588242> PMID: 7588242.
160. Haugk KL, Wilson H-MP, Swisshelm K, Quinn LS. Insulin-like growth factor (IGF)-binding protein-related protein-1: an autocrine/paracrine factor that inhibits skeletal myoblast differentiation but permits proliferation in response to IGF. *Endocrinology*. 2000; 141(1):100–10. <https://doi.org/10.1210/endo.141.1.7235> PMID: 10614628.
161. Damon SE, Haugk KL, Swisshelm K, Quinn LS. Developmental regulation of Mac25/insulin-like growth factor-binding protein-7 expression in skeletal myogenesis. *Exp Cell Res*. 1997; 237(1):192–5. <https://doi.org/10.1006/excr.1997.3787>. PMID: 9417882
162. Fatica A, Bozzoni I. Long non-coding RNAs: new players in cell differentiation and development. *Nat Rev Genet*. 2014; 15(1):7–21. <https://doi.org/10.1038/nrg3606> PubMed PMID: WOS:000328892200009. PMID: 24296535
163. Batista PJ, Chang HY. Long noncoding RNAs: cellular address codes in development and disease. *Cell*. 2013; 152(6):1298–307. <https://doi.org/10.1016/j.cell.2013.02.012> PubMed PMID: WOS:000316192500011. PMID: 23498938
164. Santoro F, Barlow DP. Developmental control of imprinted expression by macro non-coding RNAs. *Semin Cell Dev Biol*. 2011; 22(4):328–35. <https://doi.org/10.1016/j.semcdb.2011.02.018> PubMed PMID: WOS:000295212900002. PMID: 21333747
165. Gabory A, Jammes H, Dandolo L. The *H19* locus: Role of an imprinted non-coding RNA in growth and development. *Bioessays*. 2010; 32(6):473–80. <https://doi.org/10.1002/bies.200900170> PubMed PMID: WOS:000278709500005. PMID: 20486133
166. Dey BK, Pfeifer K, Dutta A. The *H19* long noncoding RNA gives rise to microRNAs miR-675-3p and miR-675-5p to promote skeletal muscle differentiation and regeneration. *Genes Dev*. 2014; 28(5):491–501. <https://doi.org/10.1101/gad.234419.113> PMID: 24532688
167. Varrault A, Gueydan C, Delalbre A, Bellmann A, Houssami S, Aknin C, et al. *Zac1* regulates an imprinted gene network critically involved in the control of embryonic growth. *Dev Cell*. 2006; 11(5):711–22. <https://doi.org/10.1016/j.devcel.2006.09.003>. PMID: 17084362

168. Gabory A, Ripoche M-A, Le Digarcher A, Watrin Fo, Ziyayat A, Forné T, et al. *H19* acts as a trans regulator of the imprinted gene network controlling growth in mice. *Development*. 2009; 136(20):3413–21. <https://doi.org/10.1242/dev.036061> PMID: 19762426
169. Merckenschlager M, Odom Duncan T. CTCF and cohesin: linking gene regulatory elements with their targets. *Cell*. 2013; 152(6):1285–97. <https://doi.org/10.1016/j.cell.2013.02.029> PMID: 23498937
170. Ma N, Zhou L, Zhang Y, Jiang Y, Gao X. Intragenic microRNA and long non-coding RNA: novel potential regulator of *IGF2-H19* imprinting region. *Evol Dev*. 2014; 16(1):1–2. <https://doi.org/10.1111/ede.12057> PMID: 24393462
171. Nordin M, Bergman D, Halje M, Engström W, Ward A. Epigenetic regulation of the *Igf2/H19* gene cluster. *Cell Prolif*. 2014; 47(3):189–99. <https://doi.org/10.1111/cpr.12106> PMID: 24738971
172. Lee RSF, Depree KM, Davey HW. The sheep (*Ovis aries*) *H19* gene: genomic structure and expression patterns, from the preimplantation embryo to adulthood. *Gene*. 2002; 301:67–77. PMID: 12490325
173. Lustig O, Ariel I, Ilan J, Lev-Lehman E, De-Groot N, Hochberg A. Expression of the imprinted gene *H19* in the human fetus. *Mol Reprod Dev*. 1994; 38(3):239–46. <https://doi.org/10.1002/mrd.1080380302> PMID: 7917273
174. Braidotti G, Baubec T, Pauler F, Seidl C, Smrzka O, Stricker S, et al. The *Air* noncoding RNA: An imprinted cis-silencing transcript. *Cold Spring Harb Symp Quant Biol*. 2004; 69:55–66. <https://doi.org/10.1101/sqb.2004.69.55> PubMed PMID: WOS:000232227200008. PMID: 16117633
175. Sleutels F, Zwart R, Barlow DP. The non-coding *Air* RNA is required for silencing autosomal imprinted genes. *Nature*. 2002; 415(6873):810–3. PubMed PMID: ISI:000173833900051. <https://doi.org/10.1038/415810a> PMID: 11845212
176. Beall MH, van den Wijngaard JPHM, van Gemert MJC, Ross MG. Amniotic fluid water dynamics. *Placenta*. 2007; 28(8–9):816–23. <https://doi.org/10.1016/j.placenta.2006.11.009> PMID: 17254633
177. van Otterlo LC, Wladimiroff JW, Wallenburg HCS. Relationship between fetal urine production and amniotic fluid volume in normal pregnancy and pregnancy complicated by diabetes. *BJOG*. 1977; 84(3):205–9. <https://doi.org/10.1111/j.1471-0528.1977.tb12556.x>
178. Merimee TJ, Grant M, Tyson JE. Insulin-like growth factors in amniotic fluid. *J Clin Endocrinol Metab*. 1984; 59(4):752–5. <https://doi.org/10.1210/jcem-59-4-752> PMID: 6384254
179. Tomoda S, Brace RA, Longo LD. Amniotic fluid volume and fetal swallowing rate in sheep. *Am J Physiol Regul Integr Comp Physiol*. 1985; 249(1):R133–R8.
180. Bloomfield FH, Breier BH, Harding JE. Fate of 125I-IGF-I administered into the amniotic fluid of late-gestation fetal sheep. *Pediatr Res*. 2002; 51(3):361–9. <https://doi.org/10.1203/00006450-200203000-00016> PMID: 11861943
181. Holt RIG. Fetal programming of the growth hormone–insulin-like growth factor axis. *Trends Endocrinol Metab*. 2002; 13(9):392–7. [https://doi.org/10.1016/S1043-2760\(02\)00697-5](https://doi.org/10.1016/S1043-2760(02)00697-5) PMID: 12367821
182. Le Roith D, Bondy C, Yakar S, Liu J-L, Butler A. The somatomedin hypothesis: 2001. *Endocr Rev*. 2001; 22(1):53–74. <https://doi.org/10.1210/edrv.22.1.0419> PMID: 11159816
183. LeRoith D, McGuinness M, Shemer J, Stannard B, Lanau F, Faria TN, et al. Insulin-like growth factors. *Neurosignals*. 1992; 1(4):173–81.
184. Young LE. Imprinting of genes and the Barker hypothesis. *Twin Res*. 2012; 4(5):307–17. Epub 02/01. <https://doi.org/10.1375/twin.4.5.307>
185. Vickers MH. Early life nutrition, epigenetics and programming of later life disease. *Nutrients*. 2014; 6(6):2165–78. <https://doi.org/10.3390/nu6062165> PubMed PMID: WOS:000338192000003. PMID: 24892374
186. Borel C, Antonarakis SE. Functional genetic variation of human miRNAs and phenotypic consequences. *Mamm Genome*. 2008; 19(7–8):503–9. <https://doi.org/10.1007/s00335-008-9137-6> PubMed PMID: WOS:000261180800004. PMID: 18787897
187. Chango A, Pogribny I. Considering maternal dietary modulators for epigenetic regulation and programming of the fetal epigenome. *Nutrients*. 2015; 7(4):2748. PubMed PMID: <https://doi.org/10.3390/nu7042748> PMID: 25875118